의학박사 학위논문

# 3D printed kagome 구조의 PCL scaffold 를 이용한 onlay 형태의 골이식

## Bone augmentation of onlay graft on rat calvaria using 3D printed kagome-structure PCL scaffold

울산대학교대학원

의 학 과

구 정 귀

# 3D printed kagome 구조의 PCL scaffold 를 이용한 onlay 형태의 골이식

지도교수 이 부 규

이 논문을 의학박사 학위 논문으로 제출함

2020 년 08 월

울산대학교 대학원
의 학 과
구 정 귀

구정귀의 의학박사학위 논문을 인준함

심사위원 황창모 

심사위원 이부규 

심사위원 김영균 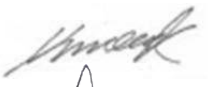

심사위원 조영삼 

심사위원 박용두 

울 산 대 학 교 대 학 원

2020 년 08 월

**Summary**

A bone graft has been widely operated for various propose such as cosmetics and reconstruction of the defect. However, onlay graft (one-wall defect reconstruction) is still challenging due to poor blood supply and insufficient graft stability. Many tissue engineering researches have been conducted for developing alloplastic bone substitutes. But there were a few studies for application of alloplastic bone substitutes on onlay graft. In order to successful results on onlay graft, the selection both of the surgical process and bone graft material are critical points. Recently, the 3D designed kagome-structure poly ε-caprolactone (PCL) scaffold was reported to have osteoconductivity in an intra-osseous bone defect which is ideal condition for bone regeneration. In addition, this scaffold has proper mechanical stability enough to rigid fixation, precise fabrication according to 3D design, and proper biocompatibility. Therefore, this scaffold has proper characteristics to apply the onlay graft. The common problems of onlay graft are wound dehiscence due to insufficient volume of soft tissue, flap necrosis due to excessive soft tissue manage, infection from hematoma, and lack of vascularization. The aim of this study is to introduce the onlay graft surgery protocol that minimizes complications using the 3 and 6 mm height of 3D kagome-structure PCL scaffold fabricated based on curved surface of micro-CT image on rat calvarial bone, and report clinical outcome of the graft with recombinant human bone morphogenetic proteins (rhBMP-2) in the hyaluronic acid (HA) based hydrogel.

For the surgical protocol, the incision was made posterior of the scaffold to avoid lay over the scaffold. After sufficient dissection, careful decortification was made on the Bregma of rat. Four miniscrews were installation for rigid fixation of the scaffold. The experiments were divided 4 rats into the 2-, 4-, and 8-weeks sacrifice group of each height scaffold. Total 24 rats were operated in this protocol with 3 and 6 mm in height and 5 mm in diameter of cylinder types 3D kagome-structure PCL scaffold. All surgical sites were complete healed without the scaffold exposure. After the sacrifice, the scaffolds were well integrated even after removal of fixation screws. In micro-CT analysis, no bone formation was observed at 2 weeks after surgery. At 8 weeks, the new bone was grow up into the fist column layer of the scaffold with kagome-shape, and the average bone formation height was about 1.0 mm

compared with the negative control. Histologically, soft tissue and collagen fibers were filled with cavity of the scaffolds at 2 weeks. At 4 weeks, active bone formation was observed from the calvarial bone, and the new bone was observed inside the scaffold. The angiogenesis and dense collagen bundle were observed on the second column cavity of the scaffold. The collagen bundle was showed higher density in 3 mm-scaffold compared with the 6 mm-scaffold in rat calvarial bone. With regard to HA based rhBMP-2 (1.0 mg/mL), the new bone formation with angiogenesis and dense collagen bundles at 2 weeks was comparable with that of the scaffold without rhBMP-2 at 8 weeks. In particular, the 3 mm-scaffold with rhBMP-2 was showed superior bone formation results compared with 6 mm-scaffold with rhBMP-2 at postoperative 4 and 8 weeks.

According to our experimental results, the 3D-kagome PCL scaffold was showed proper mechanical property for enduring fixation and osteoconductivity for onlay graft. The Kagome PCL scaffold incorporated with HA hydrogel and rhBMP-2 was showed early bone formation at 2 weeks, comparable results with the scaffold without rhBMP-2 at 8 weeks, which indicated as suitable carrier of rhBMP-2. Further studies should be conducted for optimizing application of rhBMP-2 on this scaffold to enhancing bone regeneration capacity to the large animals.

Keyword: Bone graft, Onlay graft, PCL, rhBMP-2, Scaffold, Tissue engineering

Index

List of figure

## Introduction

### Current clinical status for onlay bone graft

Various surgical techniques have been introduced to repair maxillofacial deformities, cosmetic purpose, and severe alveolar bone defect for dental implant. The clinician should be achieved successful result within shortest time by appropriate technique, and an ideal technique should be simple and minimum invasive and less risk of complications.[1] The onlay graft for one-wall defect is still challenging and the risk of complications is high, and the onlay bone graft surgery is very sensitive depending on the procedure type and experience of the surgeon. However, not all of the augmented volume are regenerated to viable bone tissue. The onlay graft is a technique to reconstruct a one-wall defect that has blood supply mainly from the recipient bone and a little from the above soft tissue. But the soft tissue could be damaged during flap elevation process and blocked by using barrier membrane. Therefore, if a huge amount of bone graft is performed vertically or horizontally, only some bone substitutes could be remodeled to viable bone tissue and the amount could be estimated within 3 mm. The other areas would be remained immature woven bone for a long time and replaced by fibrous granulation tissue due to poor blood supply.[2] The large pressure lead to loss of grafts and risk of wound dehiscence due to simulation by masticatory muscle functions.

Autogenous bone has been considered as golden standard for bone grafts because it has osteogenetic property, infection resistant, secondary healing potential with wound dehiscence. But it also has critical disadvantages such as inevitable additional surgery, limited amount of harvest, and possibility of significant resorption. Therefore, many researchers recommend mixture with other bone substitutes and covering resorbable barrier membrane.[3-7] Many tissue engineering researches have been conducted for alternative autogenous bone. However, few clinical success have been reported in the case of using the alternative bone substitutes alone for onlay graft.[8] In particular, block-type bone substitutes were mostly showed poor results and high incidence of complications.[8-10]

For evaluating the alternative bone substitues, researchers can use scanning electron microscopy (SEM) to check the macroscopic, mesoscopic, and microscopic (surface roughness) structure at x40, x100, and x3000 magnification, respectively. The mesostructure

might play an important role by providing channels for anastomosis within the bone healing period.[11] Chemical characteristics is another considering factors. Although pH is not a crucial factor for assessing the efficacy of the grafts, knowledge of the possibilities which the alloplastic bone substitutes could have a chemically toxic, which could be generated during the manufacturing process, is one of the important factors. Ham [11] tested various alloplastic bone substitutes by pH examination. The bone substitutes showed a pH of 7.3. A pH of 7.7 to 7.8 is suitable for osteoblast activity, which is the most active at pH 8.

Currently, there was no alternative block-type bone substitutes excepting the autogenous block bone. There has not been significantly different bone regeneration capacity between the particulated and block-type autogenous bone. They are easy to harvest but require an additional technique for the stabilization of particulate type, autogenous bone grafts. On the other hand, although block type autogenous bone is easy to manipulate at augmentation, it is difficult to collect.[12] With regard to clinical situation, most clinicians have been used mixture of particulate and block type autogenous bone with other additional bone subtitutes.[13, 14] For operating with the block autogenous bone, the bone—which is harvested mainly in intraoral site—is fixed with screws after obtaining intimate contact surface on recipient bone. And particulate autogenous or other bone substitutes are packed in the surrounding empty space.[15, 16] From a principles of the bone grafts, there is a gap of 10 to 100 nm between the bone substitute and host cell but the size of the cell is thirty to hundreds of micrometers.[17] This implicates that it should be an unacceptable condition in environments with a movement or pressure on the graft site. In other words, it could be disadvantageous for inducing a stable matrix from the movement of wound areas or excessive bleeding because of an inflamed tissue.

Most surgeons have performed unilateral ramal bone harvest for moderate to severe atrophy or defects involving one to four teeth, and the iliac bone harvests have been selected for further severe defects or atrophy of the jaw.[18] Jang et al. reported the 216 patients who underwent ramal harvesting, 15.28% had sensory abnormalities immediately after surgery but no cases were observed after six to nine months. Donor site infection occurred in 8.33% with inadequate drainage after surgery and 5.56% had wound dehiscence. In 49 patients who underwent an iliac harvest, an average of 8 days of gait disturbance was observed in 24.4%

of patients. Both ramus and iliac harvests had no permanent or serious donor site complications. In the recipient site, there were also mild complications with 6.42 % with wound dehiscence, 8.27% with graft removal due to infection, and 3.67% with partial graft resorption.[12]

Autogenous bone has been controversial because it has a resorption tendency after the graft. Many studies have showed the resorption rates of between 0 and 25%.[19-22] Cordaro et al. reported that up to 42% were resorbed vertically 6 months after transplantation.[20] Similar to previous studies, Lee et al.[12] reported an average 30% volume change at 1 year after the implantation of 97 implants and 0.88±0.90mm and 2.06±0.80mm of marginal bone loss were observed after 1 and 13 years, respectively. Acocella et al. reported clinical outcomes of the onlay and veneer-type block bone grafts that there were showed 0.84±1.12mm and 0.91±0.68mm of marginal bone loss, respectively, at the first year and 2.06±1.11mm and 1.26±0.60mm at 10 years after graft, respectively.[19] In 2007, A similar result was showed that most bone loss occurred in the first year. In addition, it appears to be a successful outcome based on the 2015 study, in which the progression of the bone loss was reported similar aspect of the previous research that were > 2 mm at the initial 18 months or over 0.44 mm per year.[23] Therefore, an autogenous block bone could be used reliably to improve the horizontal and vertical conditions for implant placement in moderate to severe jaw atrophy or defects. Recently, there was a successful long-term follow-up result in terms of low bone loss but there should be considering the resoprtion risk and complications of donor site.

Onlay grafts have a high risk of complication such as failure to integration, wound dehiscence, exposure of the grafts, late bone resorption and infection. To preventing such complications, the clinicians should be considered the following principles for successful onlay graft. (Table 1). [24-27]

**Table 1. The principles of onlay graft surgery success.**

| | |
|---|---|
| 1. | Adequate blood supply to the graft |
| 2. | Adequate modeling of contact surface and fixation of the block |
| 3. | Releasing incisions for a tension-free flap |
| 4. | Do not load, stimulate or compress the reconstructed area |
| 5. | Sufficient healing period to allow successful integration of the grafts |
| 6. | Avoid over-contouring with the block bone graft due to a risk of the wound dehiscence |

For successful onlay grafts, proper soft tissue healing, the surgeons should be pursued graft materials stabilization, a well-prepared recipient site with sufficient blood supply by decortification, and an infection control.[28] Among these considerations, tension-free primary closure is a critical point of the onlay graft procedure. If tension-free flap management for primary closure cannot be obtained, the wound dehiscence in the incision line and early graft exposure may inevitable.[29]. Such complications at the graft site affect the negative effect for regenerative potential of the new bone.[30, 31]

Alloplastic grafts have been used increasingly because of their excellent productivity and function as a scaffold with the development of the growth factor. Many researches have been conducted to overcome several disadvantages of autogenous bone graft. As a result, there were reported successful results with mixture of an adequate scaffold and bone growth factors such as platelet-derived growth factor (PDGF), bone morphogenetic proteins (BMP), platelet rich plasma (PRP) or platelet rich fibrin (PRF). [32-34] According to the consensus by the World Congress of Biomaterial [35], the requirement for an alloplastic graft are 1) Combination of Beta-TCP, HA, Calcium silicate 2) Interconnected macro-porosity 3) Surface micro-roughness

Conventionally, the use of an alloplastic graft has been limited only small or inlay defects due to the lack of osteogenic ability. The long-term outcome of forming functional bone needs to be researched. In particular, the particle size acts an important role in an alloplastic graft. If the size is too small, it could be affect the absorption of the adjacent tissue during the

modeling period. A size of 0.5 to 1 mm was known to be most suitable.[36] Contouring augmentation could be considered as an indication of an alloplastic bone graft for a sufficient volume. Contouring augmentation can be divided into two methods: covering with a collagen membrane or without a membrane (direct application to the graft sites without hydration). In the past, the procedure was performed mainly without a membrane, but recently, the membrane has been used widely for wound stability.[36] Even in an alloplastic graft, each graft showed different advantages according to their composition. A higher rate of bone formation was observed in particulate bone composited with collagen rather than that with a particular shape.[36] The collagen-enriched bone showed slow osteogenesis, approximately 1.5 times, but excellent volumetric stability. The application range of alloplastic bone graft has been increasing, such as ridge augmentation, in which the collagen-enriched bone covering the membrane is built up using an implant fixture as a tenting effect with a long healing period.[36]

Alloplastic grafts have been also developed in the form of block bone, which can be expected as a tenting role for large defects. It should be manufactured in such a way that allows proper mechanical stability with easy trimming, drilling, and screw fixation. Many grafts have been developed with a collagen coating for these reasons. In addition, it would be necessary to manufacture a screw type anchoring device because the fixation of the alloplastic block bone substitutes is more difficult with a conventional screw compared with autogenous block bone. A 3D printed bone substitutes have been expected if the technology advances one step further and a customized design could be available based on the micro-CT data for various bone defects. To overcome the limitations of osteogenetic property on alloplastic graft, many attempts have been to enhance bone quality by adding DNA, glycoprotein, growth factors.[36] The development of customized grafts combined with these growth factors could be the right direction. Additional accumulated data with technological development will be needed before this type of graft can be used clinically.

**Necessity and aims of tissue engineering for bone graft**

The golden standard treatment for the bone graft is still considered autologous bone which has osteogenesis, osteoinduction, and osteoconduction abilities.[37-39] To overcome several disadvantages autografts such as extended healing time and need for multiple surgeries, bone tissue engineering has been researched for temporarily substitute the extracellular matrix.

For bone tissue engineering, bone graft substitutes have been fabricated using freeze drying, solvent casting-porogen leaching, and gas foaming. But these traditional techniques cannot control the internal architecture, porosity, and geometry of the scaffold.[40] Currently, three-dimensional (3D) printing technology has rapidly becoming a promising alternative the traditional bone graft substitutes and various alloplastic scaffolds with customized shape and internal structure have been suggested.[41, 42]

Among several synthetic polymers fabrication of 3D printed scaffold, poly ε-caprolactone (PCL) is well known biodegradable polymer which has been approved by the U.S. Food and Drug Administration [43-45]. In recent study of 3-wall defect (inlay graft) with PCL scaffold, the kagome-structure showed more higher fitting ability and osteoconductivity compared with conventional grid-structure.[45] In contrast to inlay-graft which is an optimal environment for bone regeneration, still the most difficult defect to reconstruction is a 1-wall defect (onlay graft) which has limited area for proliferation of osteogenic cells and factors.[46] With regard to clinical situation, patients have been frequently required for onlay-graft, especially, in the field of implant dentistry and facial cosmetic surgery.

For successful onlay graft, the following conditions should be satisfied in terms of bone substitute (1. An intimate contact with the recipient surface, 2. Proper stiffness enduring rigid fixation, 3. Proper microstructure such as porosity for enhancing osteoconductivity, 4. No inflammatory and immunologic reaction) and surgical procedure (1. Maximize the blood circulation on the recipient site while preventing hematoma, 2. Proper flap manage for tension-free suture to avoid wound dehiscence while preventing flap necrosis caused by excessive stress, 3. Proper suture technique to prevent the animals tear the stitches by themselves.) Kim et al. suggested the new point of view in soft tissue's blood supply for the successful soft tissue healing in onlay graft surgery.[47] They reported a successful result of flap advancement by avoiding the incision which could be disturbance blood circulation.

Therefore, the author developed a novel rat model for onlay graft with securing the distance between the graft and incision area to maximize blood circulation of the soft tissue which covering above the graft.

Several members of the BMPs have been isolated, and recombinant human BMP (rhBMP-2) has been manufactured and refined for medical purposes. The U.S. FDA approved rhBMP-2, in 2007, at a concentration of 1.5 mg/mL incorporated with collagen sponge. [48]. This approved concentration, however, is $10^6$-times higher than the natural concentration in the human body. This relatively high concentration can lead side effects by increasing osteoclastic activity or oncogenecity in a cancellous bone environment. [49] Although collagen is a natural polymer, and is the most commonly used as rhBMP-2 carrier. [50-56], the rhBMP-2 from the collagen can be rapidly released by compression, diffusion and degradation of the collagen in physiological condition. To overcome these problems, many biomaterials, as carriers for rhBMP-2, have been researched in order to achieve stable localized rhBMP-2 concentrations for a sufficient period of time. [57-60] Recently, acrylated hyaluronic acid (HA) have been used as a scaffold for rhBMP-2 and human mesenchymal stem cells (hMSCs) for bone regeneration. [61] As a result, dual or sequential delivery systems—osteoconductive scaffold incorporated with rhBMP-2 into the HA-based hydrogel—can be expected to control releasing of rhBMP-2 and enhance bone formation capacity.

The aims of this study are to suggest onlay graft design using 3D printed PCL-kagome structure and surgical procedure for rat model on calvarial bone, and to evaluate bone augmentation results compared with the scaffold incorporated with rhBMP-2 in the HA-based hydrogel. The author hypothesized as below

1) There were no severe complications after the graft.
2) The Kagome PCL scaffold can endure onlay graft.
3) Intimate contact surface will obatain without soft tissue invasion.
4) New bone will grow up into the scaffold.
5) New bone formation will not different between 3 and 6 mm height scaffold.
6) The Kagome PCL scaffold with HA hydrogel will act as effective rhBMP-2 carrier

## Materials and Methods

### Design of customized PCL scaffolds using micro CT data

A kagome-structure model was fabricated as followed the previous reported studies [45, 62]. For 3D modeling of rat calvaria model, micro-CT were taken on rat calvaria (Male Sprague rats, 7 weeks of age) using a 16-slice multidetector CT scanner (SOMATOM Sensation 16, Siemens AG, Forchheim, Germany; 120 kV, 220 mA, and 0.75 mm of thickness). Axial views of 0.1 mm thickness were reconstructed with the CT scanner with an H60s medium-smooth kernel. The field of view was 100×100 mm on the Bregma (perpendicular intersection of the coronal suture and sagittal suture) and data were acquired in a 512×512 data matrix. (Figure 1)

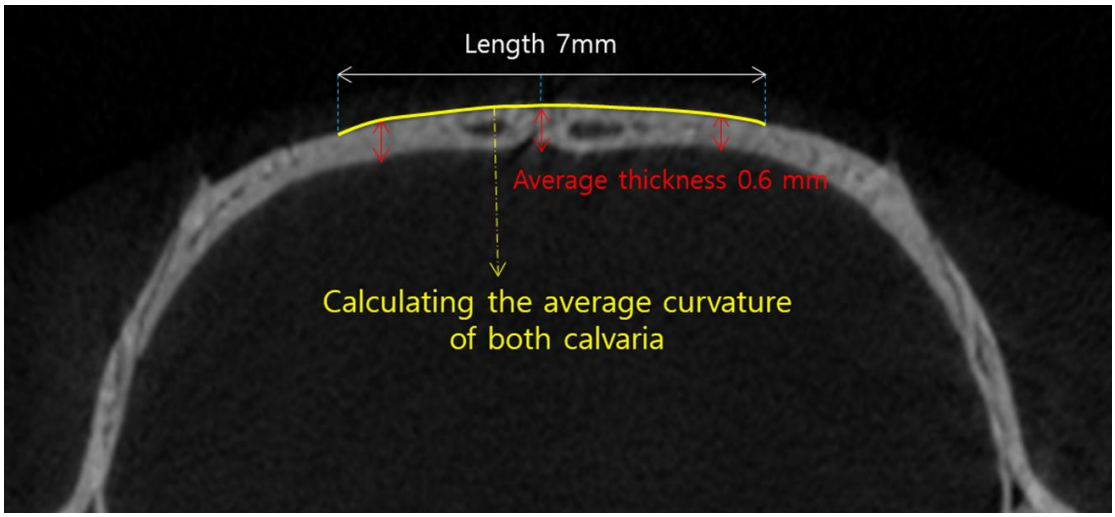


**Figure 1. Rat calvarial bone at coronal view of Bregma.**

PCL (Mn = 45 000, Tm = 60 °C, Sigma-Aldrich) was selected for the fabrication of the scaffold. Kagome-structure scaffold was designed by 3D reconstruction model using CATIA V5 R13 software (Dassault systems® CATIA, Paris, France). The kagome-structure model was cut along the outline of the calvarial contour at coronal view of Bregma of rat as shown in figure 1. The scaffold was composed of a number of kagome unit cells. The structure of the designed kagome model can be divided into regions of frames and columns. The cylinder shape scaffold was designed that had 6 mm in height and 5 mm in diameter with four side wings that had 1.2 mm in height and 3 mm in diameter and 50 % of porosity as shown in figure 2.

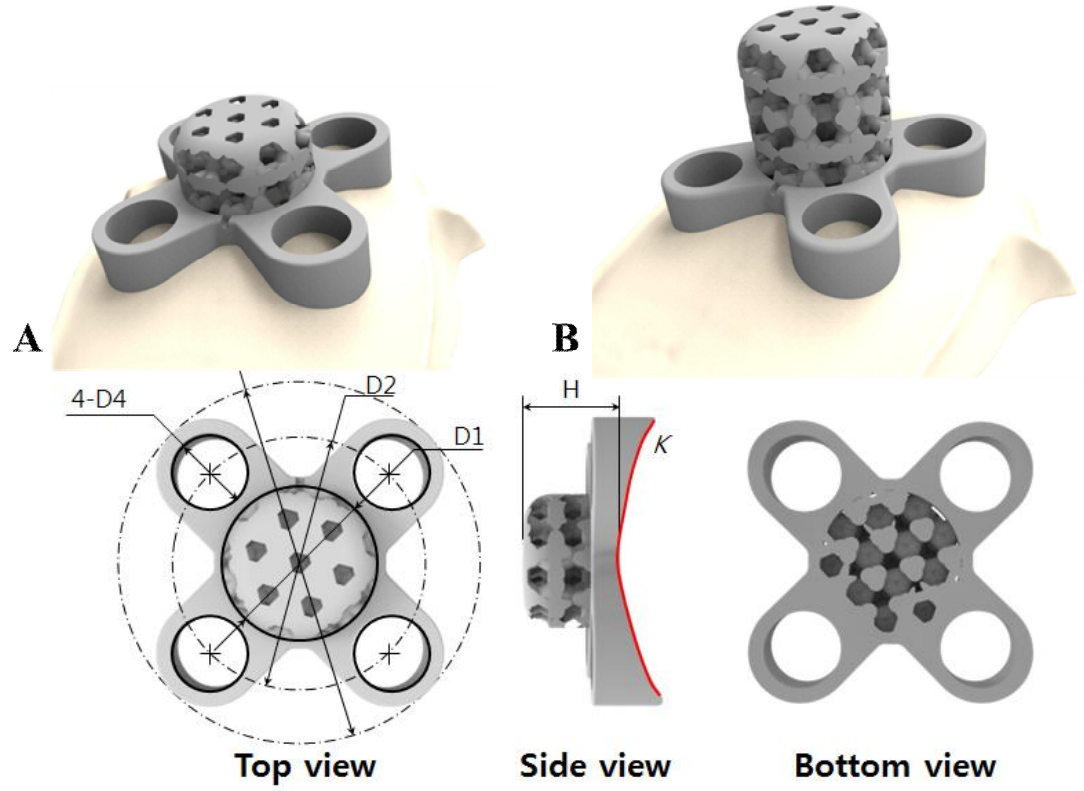


C

Unit: mm

| D1 | D2 | D3 | D4 | H | *K* |
|---|---|---|---|---|---|
| 5 | 8.6 | 12.2 | 2.6 | 3, 6 | Rat calvaria |

**Figure 2. 3D Design of customized Kagome-PCL scaffolds.** A. 3D image of a 3 mm-height scaffold. B. 3D image of a 6 mm-height scaffold. C. The design and detailed size of the scaffold.

**Fabrication of PCL scaffolds using a 3D printer with a PED head [62]**

The open-source software Slic3r (version 1.2.9) was used for a tool pathway generation of the STL model. Figures 3 A and B showed an images of the deposition process at the column part of the kagome-scaffold. Figures 3 C and D showed the deposition process at the frame part of the kagome-scaffold. The yellow lines and pink lines showed the inner filled material and outer wall in figures 3 A–D, respectively. The tool pathway was converted to operate motion program with customized software developed using Visual Basic 6.0 (Microsoft, USA). The lab-made precision 3D printer with the PED head is shown in figures 3 E. The PED head was composed of a barrel, screw, cartridge body, nozzle, gear set, fans, heating block and motor (Figures 3 F) The structural design of the PED head was improved by a parallel-type gear set and fans for cooling to minimize the thermal influence of the thermal energy transferred from the heating block on the motor. The melted material was extruded by rotating the screw with 70 rpm under an air pressure of 360 ± 5 kPa to prevent heating over 80 °C which is the melting point of PCL pellet. Several kagome-structure scaffolds were made using a ceramic nozzle with a size of 50 μm simultaneously (Figure 3 G). The extrude velocity was set as 1.15$mms^{-1}$ and feed rate was set as 1.00$mms^{-1}$ to manufacture strands with a thickness to 500 μm.

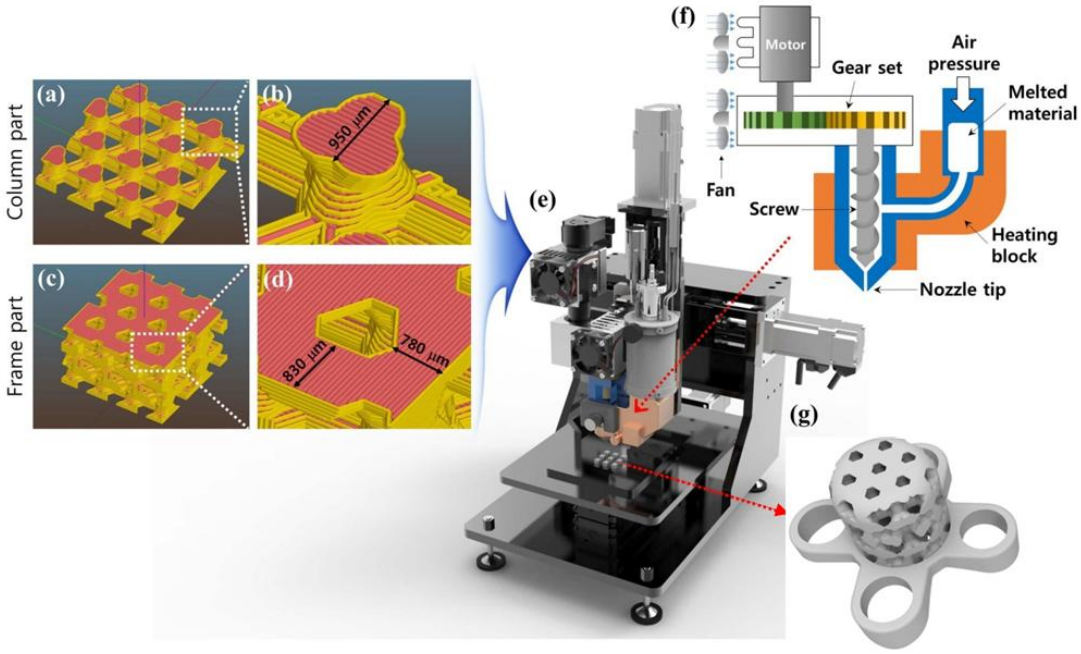


**Figure 3. 3D illustration of the kagome-structure scaffold deposited by 3D printing [62].** A. deposition process image of column region, B. magnified image of a column region, C. deposition process image of a frame region, D. magnified image of a frame region (yellow lines: outer wall, pink lines: inner filler), E. illustration of developed precision 3D printer, F. schematic of precision extruding deposition (PED) head, G. illustration of the deposition process using the precision nozzle.

**Animal preparations and surgery process for Kagome-structure PCL scaffold**

The animal procedures used in the experiment were approved by the Institutional Animal Care and Use Committee (IACUC) and followed the ethical principles for animal experimentation established by the institute.

Sample size was initially calculated at 20 animals for six experimental groups considering a significance level of 5% and a power of statistical test of 95%. But, to rationalise and distribution of animal sample we considered 24 animals. The twenty-four rats were purchased from Orientbio© (Seongnam, Korea) and divided into 6 groups (the 3 and 6 mm height of the scaffold with sacrificed at 2-, 4-, and 8-weeks, respectively). (Table 2)

**Table 2. Distribution of experimental animals**

| Male Sprague rats (7 weeks of age) | Sacrifice weeks | | |
|---|---|---|---|
| | 2 | 4 | 8 |
| 3 mm Kagome-PCL scaffold | N=4 | N=4 | N=4 |
| 6 mm Kagome-PCL scaffold | N=4 | N=4 | N=4 |
| Negative control (Decortification only) | | | N=1 |
| Second negative control (The base scaffold  ) | | | N=2 |

The rats anesthetized with tiletamline and zolazepam hydrocholoride (Zoletil 50®) and Xylazine hydrochloride (Rompun®) injected intraperitoneally 20mg per kg of body weight. The hair on surgical site was shaved and disinfected with povidone-iodine. After infiltration of 1.8 ml lidocaine (2 % lidocaine HCl, Huons, Korea) for local anesthesia, linear incision was made from distal margin of the scaffold along the sagittal line and the periosteal was anteriorly dissected to form a pocket beneath. (Figure 4 A-C) The 3-4 foramina were made for decortification with a micro-drill (2.0 mm diameter, Neo Biotec, Korea) on Bregma [63]. (Figure 4 D) After placing the scaffold on Bregma, the scaffold was fixed using 4 mm of miniscrews (2 mm diameter, Neo Biotec, Korea) on four side wings. (Figure 4 E, F) During drilling procedure, sterile saline was simultaneously irrigated the surgical site to prevent thermal damage. After flap adaptation, the scaffold was covered with non-damaged soft tissue. (Figure 4 G) The surgical site was sutured using a continuous horizontal mattress suture technique and vertical mattress suture on anterior third portion of incision line with 4-0 black silk. (Figure 4 H, I) After the experiment, ampicillin (50 mg/kg) and ketorolac tromethamine (1 mg/kg) were administrated intramuscularly twice daily for 3 days to reduce pain and to prevent infection and disinfected with povidone-iodine solution. The four rats of each group were sacrificed on 2nd, 4th and 8th weeks after surgery.

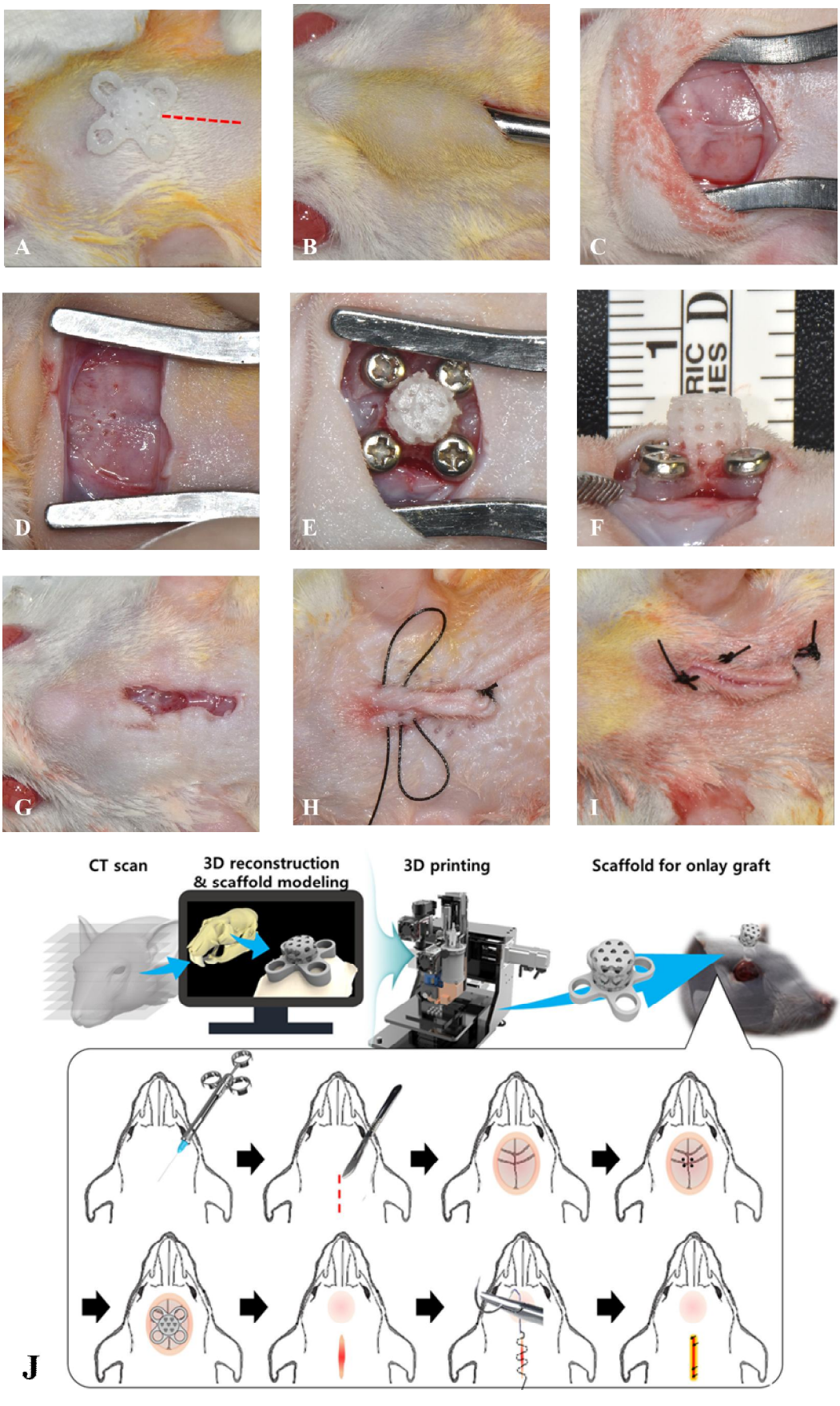
A
B
C
D
E
F
G
H
I
CT scan
3D reconstruction
& scaffold modeling
3D printing
Scaffold for onlay graft
J

**Figure 4. Process of onlay graft with 3D printed kagome-structure PCL scaffold on rat calvarial bone.** A. The incision line (red line) was performed at posterior point on the scaffold. B and C. Anteriorly dissection of periosteum flap was made toward Bregma. D. Decortification was made with three to four drilling holes on Bregma. E. The scaffold was adapted on bregma and fixed with four miniscrews. F. Lateral view of the 6 mm scaffold fixation. G Flap was fully covered the scaffold without including incision line. H and I. Continuous horizontal mattress suture and vertical mattress suture on anterior third point of the incision line were made by 4-0 black silk. J. Schematic of the onlay graft process with 3D printed kagoma-structure PCL scaffold.

**Preparations and surgery process for Kagome-structure PCL scaffold loaded with rhBMP-2 by hyaluronic acid-based hydrogel. [64, 65]**

Hyaluronic acid (HA; MW 170,000 Da) was purchased from Lifecore Biomedical Co. (Chaska, MN, USA). 1-Ethyl-3-(3-dimethylaminopropyl)-carbodimide, triethanolamine and adipic acid dihydrazide (ADH) were acquired from SigmaeAldrich (St. Louis, MO, USA). 1-hydroxybenzotriazole hydrate was purchased from Fluka Chemical (Buchs, Switzerland). N-acryloxysuccinimide was purchased from Acros Organics (Pittsburgh, PA, USA), and RGD peptides and MMP-insensitive peptides were obtained from AnyGen (Gwang-ju, Korea). Carrier-free recombinant human bone morphogenic protein (BMP)-2 was purchased from Cowell medi Co. (Busan, Korea). Fetal bovine serum (FBS), penicillin streptomycin, trypsin, and low-glucose Dulbecco's modified Eagle's medium (DMEM) were purchased from GIBCO BRL (Grand Island, NY, USA).

HA (0.25 mmol, based on the repeating unit MW) was dissolved in 40 ml of distilled water and EDC (0.24 g, 1.25 mmol), HOBT (0.17 g, 1.25 mmol) and adipic acid dihydrazide (ADH) (2.2 g, 12.5 mmol) were added to the solution [20]. The EDC mediated coupling reaction between the carboxyl group of HA and the hydrazide group of ADH continued, with stirring, at room temperature for 8 h. HA–ADH was dialyzed against 100mM NaCl for 2.5 days and distilled water for 1 day, using a dialysis membrane (MWCO14,000, SpectraPor; Rancho Dominguez, CA, USA). NAS (0.5 g, 3 mmol) was subsequently added to the HA–ADH solution. The reaction continued, with stirring, at room temperature for 12 h. HA–ADH–NAS was dialyzed extensively against 100mM NaCl for 2.5 days and distilled water for 1 day. The product was then lyophilized for 3 days to obtain solid acrylated HA (HA-Ac). The NMR spectra were obtained on a Mercury 200 NMR (200MHz) from Varian (Lake Forest, CA, USA). D2O was used as a solvent for all the samples and the reported spectra represented an average of 64 scans. The degree of acrylation was calculated by comparing peaks from the acryl and methyl groups from the HA residue.

For gel preparation, matrix-metalloproteinase (MMP)-sensitive peptides (GCRDGPQGIWGQDRCG) or MMPinsensitive peptides (GCRDGDQGIAGFDRCG) were added to acrylated HA solution with the same molar ratio of acryl and thiol groups.[64] Acrylated HA was dissolved in a triethanolamine-buffered solution (TEA; 0.3 M, pH 8).

PEG-SH4 (MW 10,000) was added as a cross-linker with the same molar ratio of acryl and thiol groups. HA-based hydrogel was formed via a Michael-type addition reaction [66]. The reaction mixture was incubated at 37.1C for gelation. This hydrogel (5% wt of HA and PEG-SH4) was set as 1.0 ug/uL of rhBMP-2 and used in both *in vivo* experiments. (Table 2) Before complete gelation, the HA–based hydrogel incorporated with rhBMP-2 was loaded into the scaffold. (Figure 5)

**Table 2. The proportion of hyaluronic acid-based hydrogel incorporated with rhBMP-2**

| | A kagome-scaffold | |
|---|---|---|
| | 3 mm height | 6 mm height |
| Total cavity volume | 35 uL | 56 uL |
| Hyaluronic acid | 31.5 uL | 50.4 uL |
| Matrix-metalloproteinase | 0.45 mg/3.15 uL | 0.72 mg/5.04 uL |
| recombinant human bone morphogenic protein-2 | 0.35 ug/ 0.35 uL | 0.56 ug/0.56 uL |

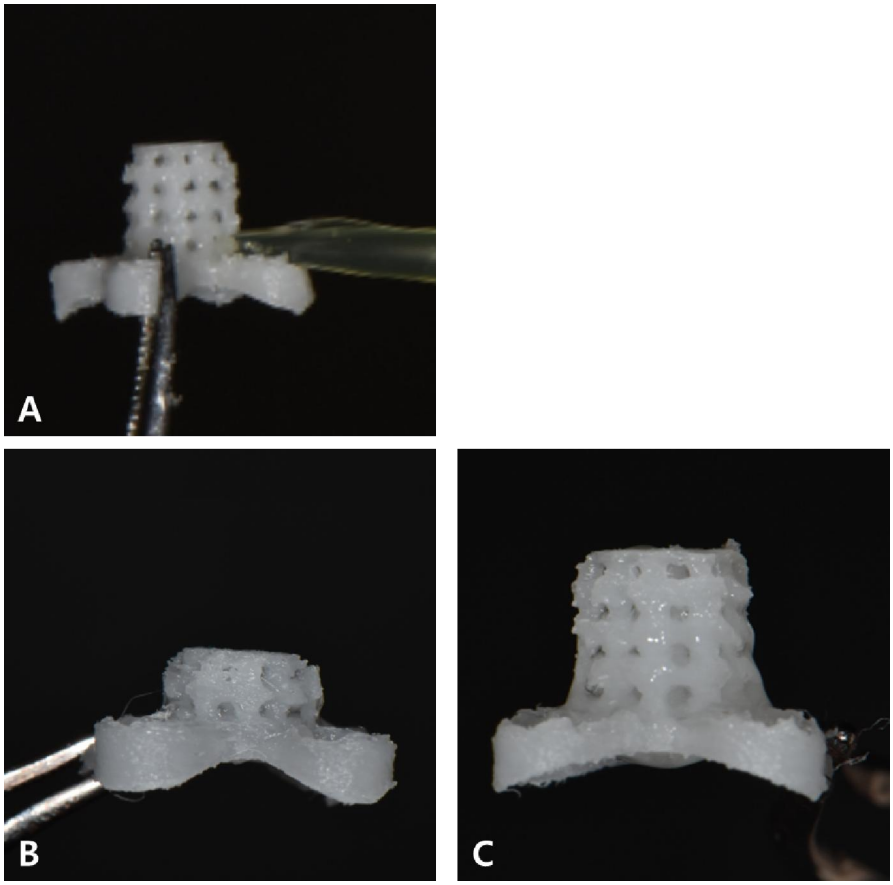


**Figure 5. The HA–based hydrogel incorporated with rhBMP-2** A. The HA–based hydrogel incorporated with rhBMP-2 was loaded into the scaffold. B. The 3 mm Kagome-PCL scaffold with rhBMP-2. C. The 6 mm Kagome-PCL scaffold with rhBMP-2

**Analysis of the experiment results on micro-CT**

After sacrifice, the scaffold was carefully excised *en block* with calvarial bone by using saw after incision and dissection of skin and subcutaneous tissue. The removed tissues were immediately fixed with 4% (w/v) paraformaldehyde for 5 days. The grafts were removed the fixation screws and after sacrifice. Micro-CT was taken with 16-slice multi-detector CT scanner (SOMATOM Sensation 16, Siemens AG, Forchheim, Germany; 120 kV, 220 mA, and 0.75 mm of thickness). Fixed specimens were wrapped with parafilm to minimize drying. The specimens were scanned by micro-CT (SkyScan 1176, Kontich, Belgium) at a high resolution with an aluminum filter (0.5 mm). Scan settings were as follows: resolution of 35.76-μm pixels, energy of 50 kV, and intensity of 500 μA. Projection images of CT scan and reconstruction were saved as 16-bit TIFF files. The image files were transferred to set the measurement software (ImageJ, National Institutes of Health, USA), and the bone height was measured between the highest point of the new bone inside the scaffold and the perpendicular point of the calvarial base. (Figure 6A) For the comparison, two rats were implanted the base scaffold for 8 weeks as the base scaffold group (Figure 6 B) and other one rat was operated only decortification drilling without scaffold implantation as the negative control group.

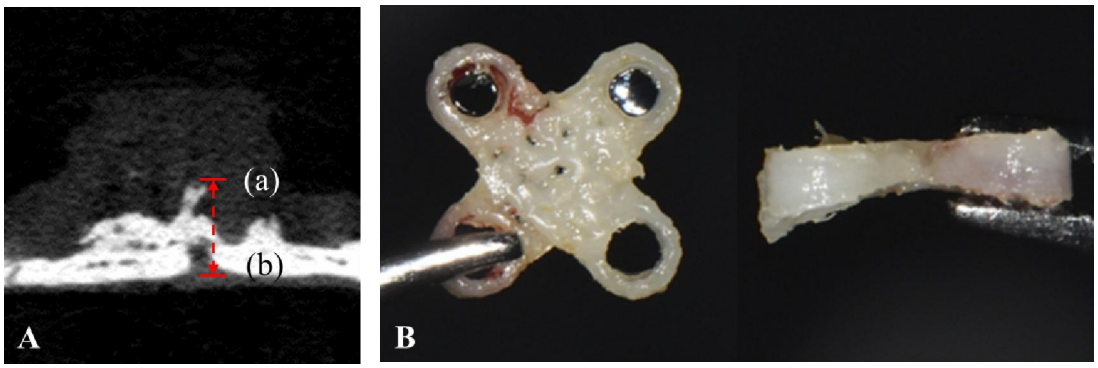


**Figure 6. The measurement of bone height inside the scaffold.** A. The measurement of bone height inside the scaffold. (a; The highest point of the new bone inside the scaffold, b: The perpendicular point of the calvarial base from (a) point) B. For the comparison, additional two rats were implanted the base scaffold for 8 weeks.

**Histological analysis of the experiment**

After micro-CT acquisition, decalcification was performed by 10% ethylenediaminetetraacetic acid (EDTA) for 14 days at room temperature. The prepared samples were embedded in paraffin after dehydration. The coronal sections (5 μm in thickness) were made and stained with hematoxylin and eosin (H&E) and Masson's Goldner trichrome (MT) methods to evaluate the angiogenesis, new bone formation, and spatial gap between the scaffold and calvarial bone.

The H&E staining was follow the below procedure. 1) Deparaffinize sections, 2 changes of xylene, 10 minutes each. 2) Re-hydrate in 2 changes of absolute alcohol, 5 minutes each. 3) 95% alcohol for 2 minutes and 70% alcohol for 2 miuntes. 4) Wash briefly in distilled water. 5) Stain in Harris hematoxylin solution (Hematoxylin, H9627, Sigma-Aldrich, USA) for 8 minutes. 6) Wash in running tap water for 5 minutes. 7) Differentiate in 1% acid alcohol for 30 seconds. 8) Wash running tap water for 1 minute. 9) Bluing in 0.2% ammonia water or saturated lithium carbonate solution for 30 seconds to 1 minute. 10) Wash in running tap water for 5 minutes. 14) Rinse in 95% alcohol, 12 dips. 15) Counterstain in eosin-phloxine solution for 30 seconds to 1 minute. 16) Dehydrate through 95% alcohol, 2 changes of absolute alcohol, 5 minutes each. 17) Clear in 2 changes of xylene, 5 minutes each. 18) Mount with xylene based mounting medium

The MT staining was follow the below procedure**.** 1) Deparaffinize and rehydrate through 100% alcohol, 95% alcohol 70% alcohol. 2) Wash in distilled water. 3) For Formalin fixed tissue, re-fix in Bouin's solution for 1 hour at 56 C to improve staining quality although this step is not absolutely necessary. 4) Rinse running tap hot water for 30 minutes to remove the yellow color. 5) Stain in Weigert's iron hematoxylin (H9627, Sigma-Aldrich, USA; Iron III chloride, I0446, Samchun, Korea) working solution for 10 minutes. 6) Rinse in running the warm tap water for 10 minutes. 7) Wash in distilled water. 8) Stain in Biebrich scarlet-acid fuchsin (F8129, Sigma-Aldrich, USA) solution for 10-15 minutes. Solution can be saved for future use. 9) Wash in distilled water. 10) Differentiate in phosphomolybdic-phosphotungstic acid solution (Phosphomolybdic acid, P0434, Samchun, Korea; Phosphotungstic acid, F4006,

Sigma-Aldrich, USA) for 15 minutes or until collagen is not red. 11) Transfer sections directly (without rinse) to aniline blue solution (A1475, Samchun, Korea) and stain for 10 minutes. Rinse briefly in distilled water and differentiate in 1% acetic acid solution for 3 minutes. 12) Wash in distilled water. 13) Dehydrate very quickly through 95% ethyl alcohol, absolute ethyl alcohol (these step will wipe off Biebrich scarlet-acid fuchsin staining) and clear in xylene. 14) Mount with resinous mounting medium.

**Statistical analysis**

All data were expressed as the mean ± standard deviation. Statistical analysis was performed on the micro-CT results using single factor analysis of variance with SPSS version 25.0 software (SPSS, Inc., Chicago, IL, USA), and a significance was considered at 0.05 level.

**Results**

The 3D printed kagome-structure PCL scaffolds were fabricated for intimate surface fit. Twenty-three experimental animals showed no dehiscence and hematoma during observation period (Figure 7 A-C). One rat was showed wound dehiscence without the 3-mm scaffold exposure at three days after surgery, but it was observed secondary healing well without dislodgement of the scaffold during 4-weeks. (Figure 7 D-F)

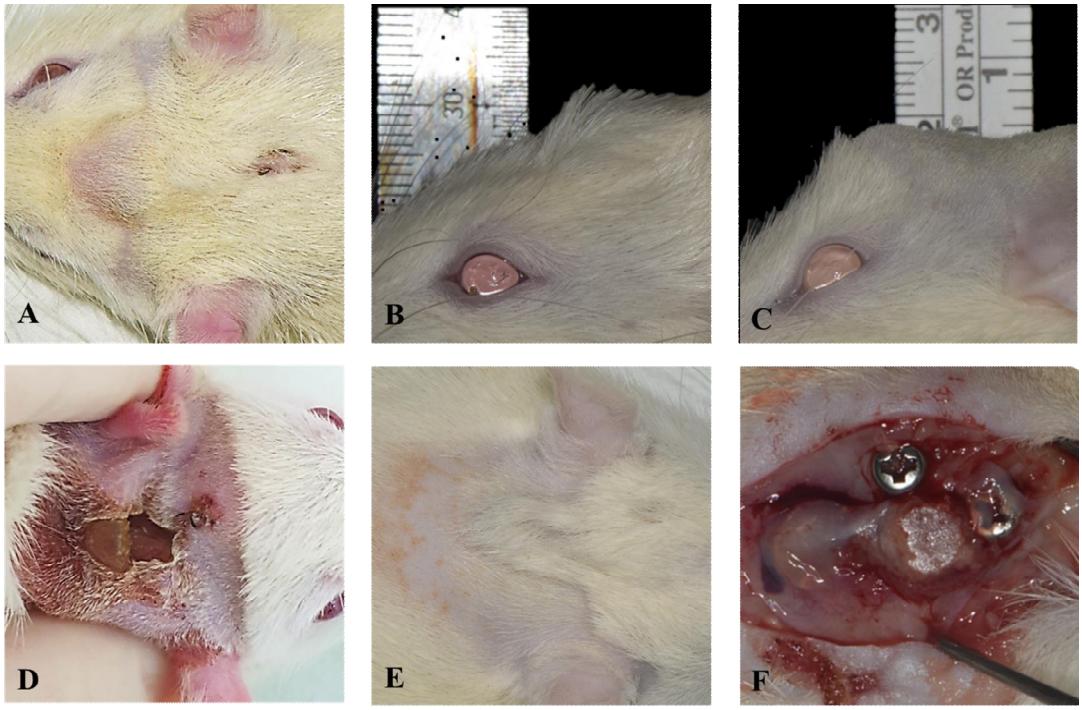


**Figure 7. Clincial photographs after surgery**. A. Complete healing of incision sites of the 23 rats without wound dehiscence at 2 weeks. B. Lateral view of the rat with 3 mm scaffold. C. Lateral view of the rat with 6mm scaffold D. At 3 days after surgery, a rat with the 3 mm scaffold was showed wound dehiscence without scaffold exposure. E. The dehiscence rat was observed secondary healing at postoperative 4 weeks F. Excessive fibrous tissue was covered on posterior of the scaffold and the scaffold was well integrated.

With regarding clinical aspects at sacrifice, all scaffolds were well integrated from calvarial bone with fibrous tissue coverage and removal of all fixation screws at 2-, 4-, and 8-weeks. (Figure 8 and 9)

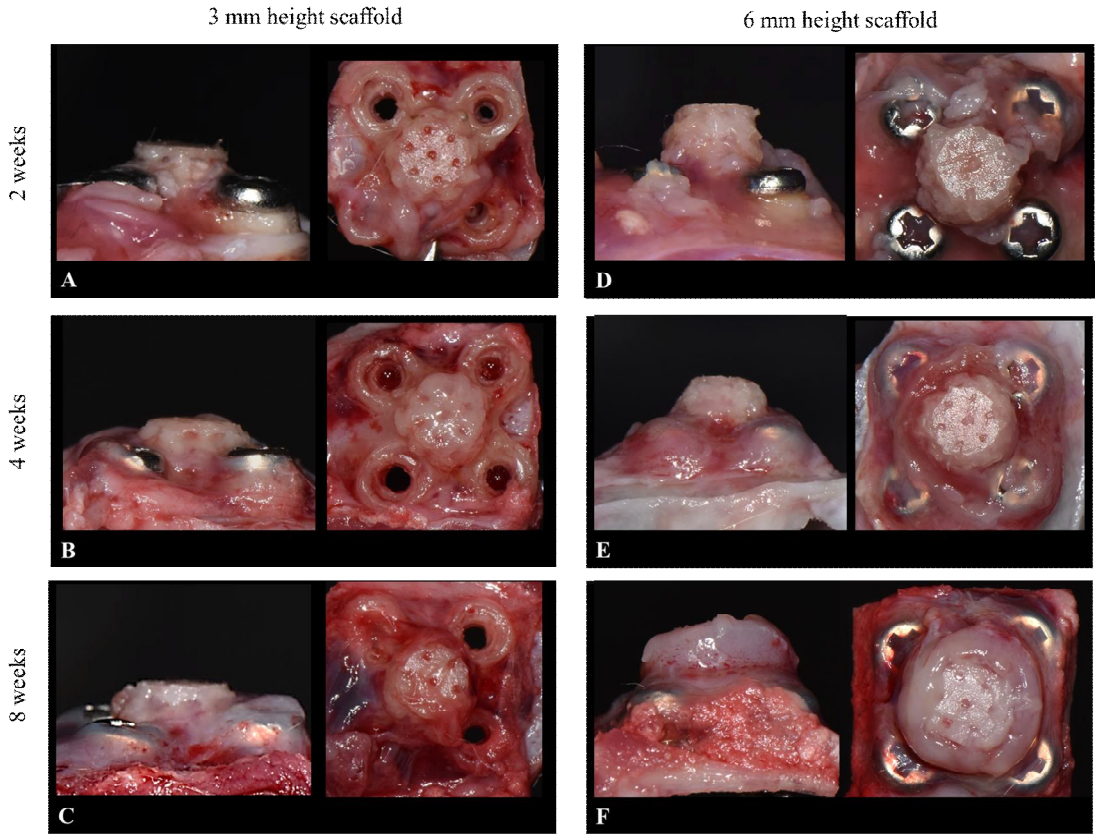


**Figure 8. The grafts after the sacrifices and removal of all fixation screw.** The scaffolds were covered with fibrous tissue and well integrated from calvarial bone. A. The 3 mm-height scaffold sacrificed at 2 weeks after surgery. B. The 3 mm-height scaffold sacrificed at 4 weeks. C. The 3 mm-scaffold sacrificed at 8 weeks. D. The 6 mm-height scaffold sacrificed at 2 weeks after surgery. E. The 6 mm-height scaffold sacrificed at 4 weeks. F. The 6 mm-scaffold sacrificed at 8 weeks.

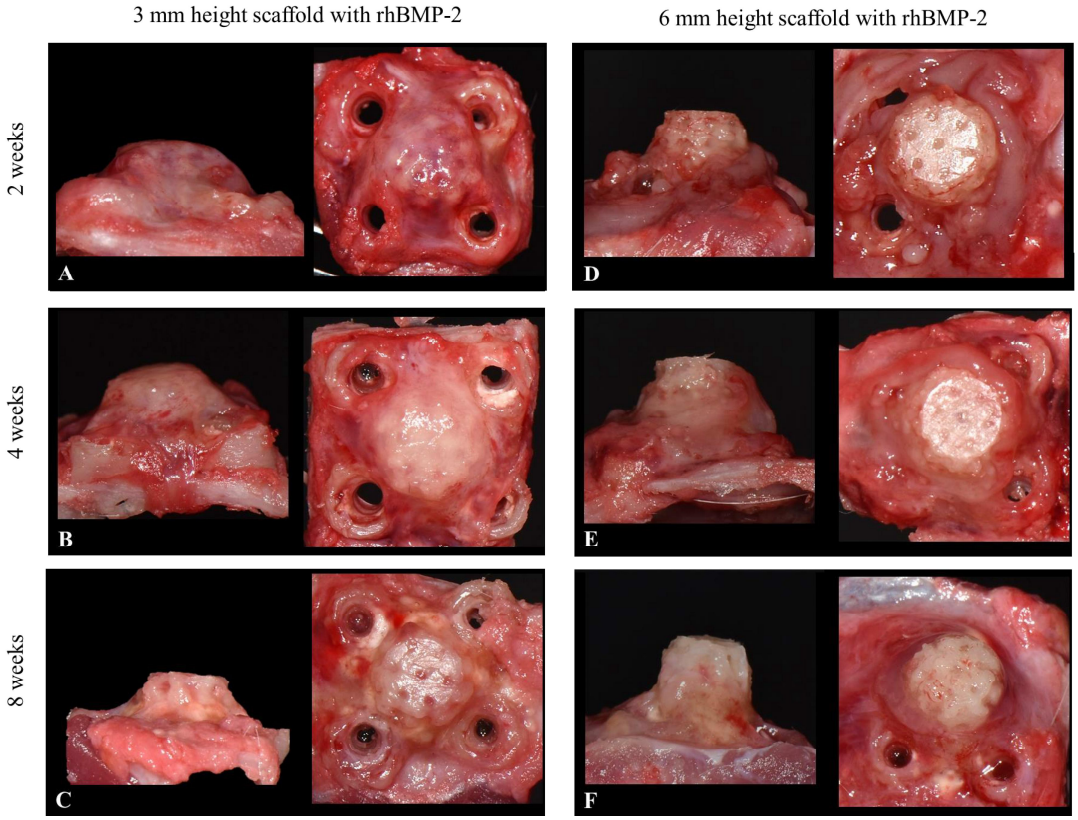


**Figure 9. The grafts with rhBMP-2 after the sacrifices and removal of all fixation screw.** The scaffolds with rhBMP-2 were covered with fibrous tissue and well integrated from calvarial bone. A. The 3 mm-height scaffold with rhBMP-2 sacrificed at 2 weeks after surgery. B. The 3 mm-height scaffold with rhBMP-2 sacrificed at 4 weeks. C. The 3 mm-scaffold with rhBMP-2 sacrificed at 8 weeks. D. The 6 mm-height scaffold with rhBMP-2 sacrificed at 2 weeks after surgery. E. The 6 mm-height scaffold with rhBMP-2 sacrificed at 4 weeks. F. The 6 mm-scaffold with rhBMP-2 sacrificed at 8 weeks.

**Micro-CT results**

We used Asan J software (Asan Medical Center, Seoul, Korea) based on Image J (NIH, Bethesda, MD, USA) to analyze bone formation using CT images. Overall, the 3 and 6 mm scaffolds were showed similar bone formation aspect depending on the healing period. (Figure 10) The new bone growth was not observed toward the 3 and 6 mm scaffolds on Bregma at 2 weeks. At 4 weeks, a bone growth was observed into the middle portion of the 3 and 6 mm scaffolds. At 8 weeks, the bone regeneration was grow up into the first column cavity of the 3 and 6 mm scaffolds, and was showed a kagome-shape new bone in axial view. (Figure 10 A) On the other hands, the new bone was formed at 2 weeks inside the scaffold with rhBMP-2, and was showed a kagome-shape new bone in axial view. At 4 weeks, the bone growth was dominantly observed in the 3 mm scaffold with rhBMP-2. At 8 weeks, the bone regeneration was grow up into the second column cavity of the 3 and 6 mm scaffolds with rhBMP-2. (Figure 10 B) The new bone formation was dominantly greater than the negative controls. (Figure 10 C)

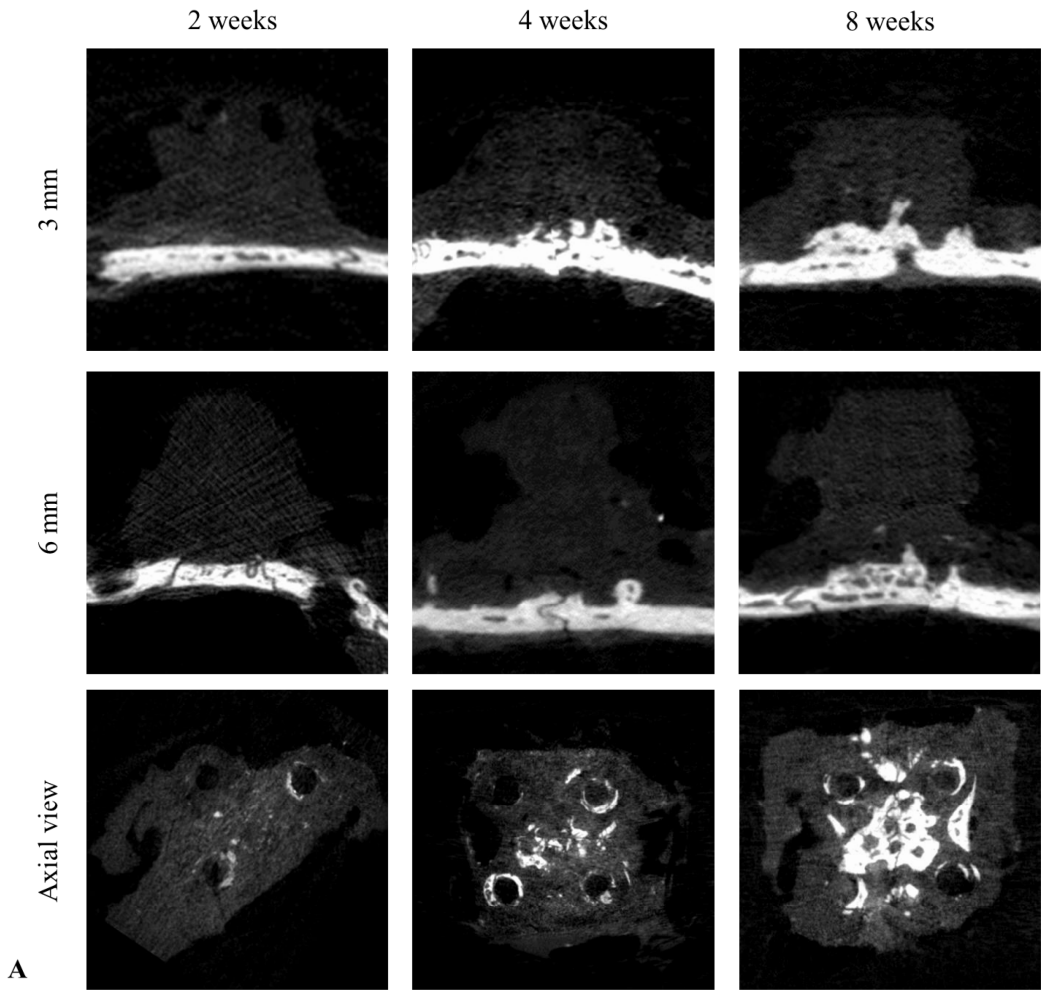


**A**

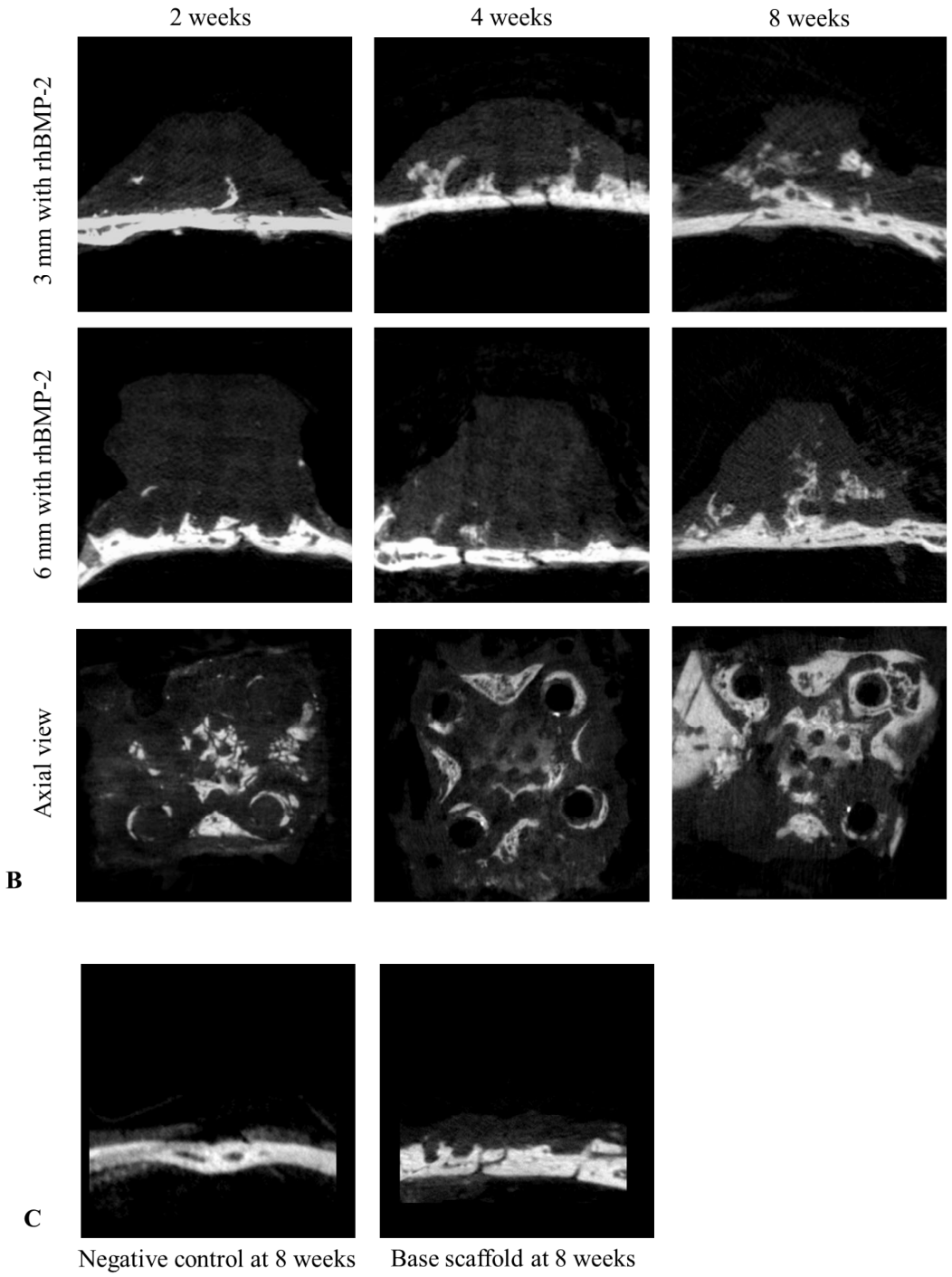


**Figure 10. MicroCT images of onlay graft with 6 mm height 3D printed kagome-structure PCL scaffold.** A. The 3 and 6 mm height scaffold. There was not observed new bone formation at 2 weeks. At 4 weeks, new bone formation was slightly observed inside the scaffold. At 8 weeks, new bone formation was observed almost entired first column

cavity. The axial view of the scaffold was showed the Kagoma-shape new bone formation in the scaffold at 8 week. B. The 3 and 6 mm height scaffold with rhBMP-2. At 2 weeks, new bone formation was slightly observed inside the scaffold, and the aspect was superior than the scaffold without rhBMP-2 at 4 week. At 4 weeks of the scaffold with rhBMP-2, new bone formation was observed almost entired first column cavity of 3-mm scaffold. At 8 weeks, new bone formation was observed almost entired second column cavity of the scaffold. The axial view of the scaffold was showed the Kagoma-shape new bone formation in the scaffold from 2 week postoperatively. C. The negative control and the base scaffold group (second negative control) at 8 weeks.

The average bone height of 3 mm scaffolds were 0.65 ± 0.10, 1.25 ± 0.21, and 2.13 ± 0.30 mm at 2, 4, and 8 weeks, respectively. And the average bone height of 6 mm scaffolds was 0.77 ± 0.06, 1.08 ± 0.05, and 1.73 ± 0.40 mm at 2, 4, and 8 weeks, respectively. At 8 weeks, the mean bone height of 3 mm-scaffold was higher than that of the negative control group (1.00 mm, P=0.036) and the base scaffold group (1.40 ± 0.14 mm, P=0.044). (Figure 11 A) The average bone height of total scaffolds was 0.70 ± 0.10, 1.55 ± 0.43, and 1.96 ± 0.38 mm at 2, 4, and 8 weeks, respectively. At 8 weeks, the mean bone height of total scaffolds was higher than that of the negative control group (P=0.001) and the base scaffold group (P=0.02). (Figure 11 B)

To evaluate the bone height compared with the basal bone, the bone height percentage was calculated based on the mean calvarial bone thickness of 7-weeks rat (0.6 mm). The average bone height percentage of 3 mm scaffolds were 108.3 ± 16.7, 208.3 ± 34.7, and 354.1 ± 49.8% at 2, 4, and 8 weeks, respectively. And the average bone height percentage of 6 mm scaffolds was 127.8 ± 9.62, 179.2±8.33, and 288.9 ± 67.4% at 2, 4, and 8 weeks, respectively. At 8 weeks, the mean bone height of 3 mm-scaffold was higher than that of the negative control group (167.0%, P=0.005) and the base scaffold group (233.5 ± 23.3%, P=0.035). (Figure 11 C) The average bone height percentage of total scaffolds was 116.7 ± 16.7, 258.3 ± 72.1, and 326.2 ± 63.0 mm at 2, 4, and 8 weeks, respectively. At 8 weeks, the mean bone height percentage of total scaffolds was higher than that of the negative control group (P=0.001) and the base scaffold group (P=0.006). (Figure 11 D)

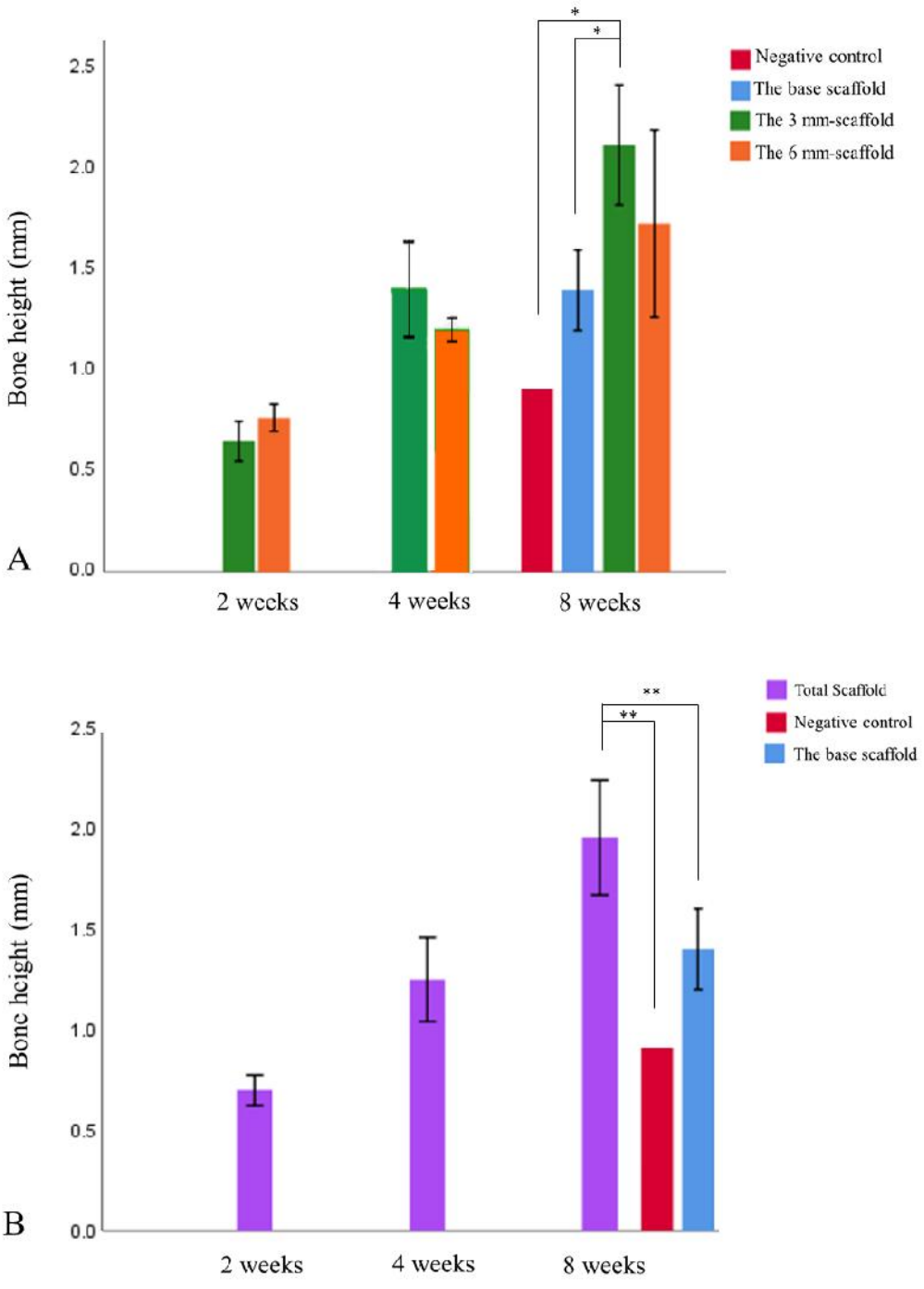
A
Bone height (mm)
2.5
2.0
1.5
1.0
0.5
0.0
*
*
Negative control
The base scaffold
The 3 mm-scaffold
The 6 mm-scaffold
2 weeks
4 weeks
8 weeks
B
Bone height (mm)
2.5
2.0
1.5
1.0
0.5
0.0
**
**
Total Scaffold
Negative control
The base scaffold
2 weeks
4 weeks
8 weeks

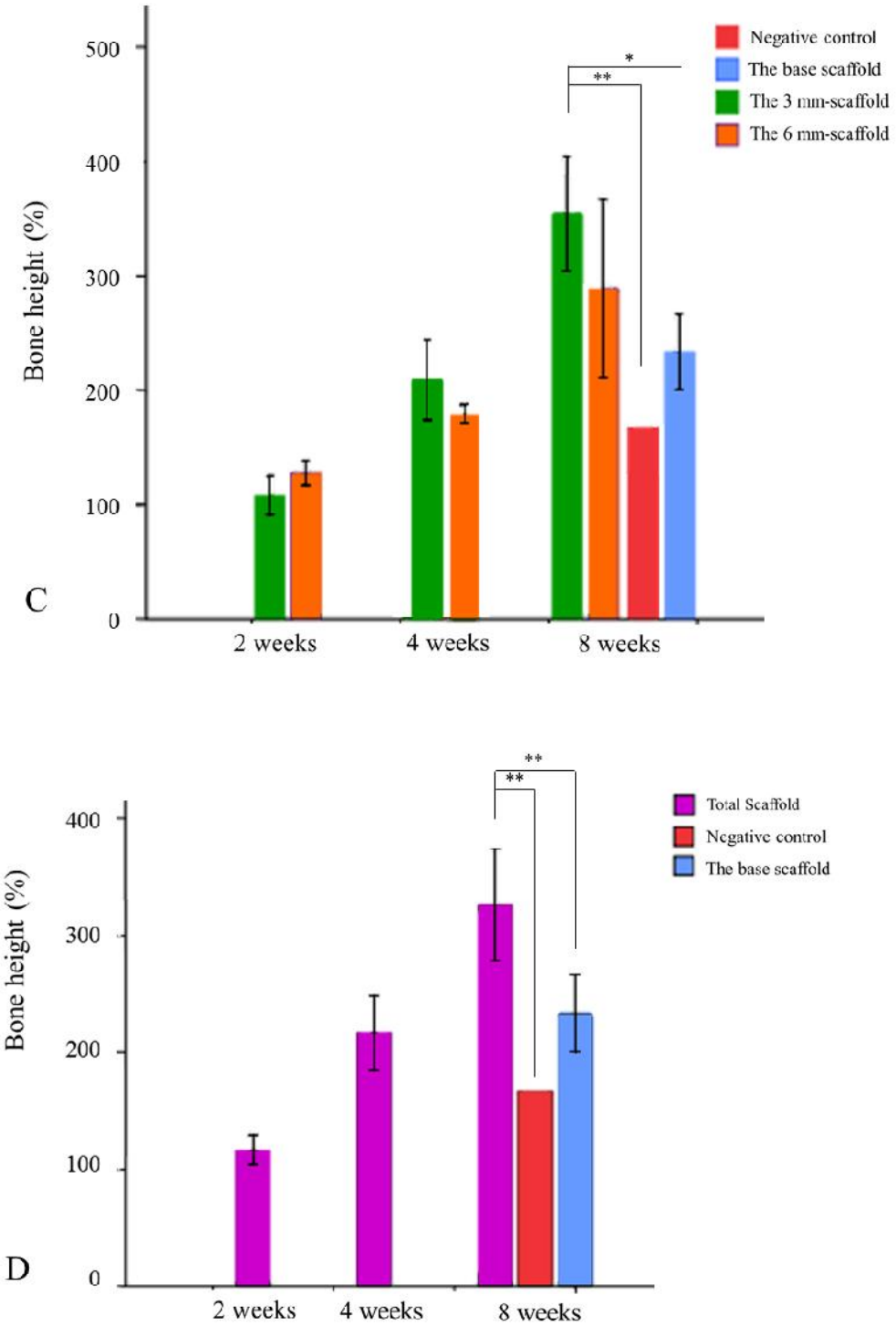


**Figure 11. The mean bone height which was calculated between the highest bone level inside the scaffold from the calvarial bone.** A. The bone height according to each group. B. The bone height of the total scaffolds and the negative groups. C. The bone height

percentage based on the calvarial bone thickness of 7-weeks age rat (0.6 mm) according to each group. D. The bone height percentage of the total scaffolds and the negative groups based on the calvarial bone thickness of 7-weeks age rat (0.6 mm). (*P < 0.05, **P < 0.01)

**Histologic results**

A closed contact was formed between the scaffold and the calvarial bone that could not allow to invasion any soft tissue into the surface. Fibrous tissues were integrated from the lateral and coronal side of the scaffold. The new bone formation was observed from the calvarial bone below the scaffold, and the active bone remodeling was showed around the decortificated holes. At 2 weeks, the cavity of the scaffold was filled with fibrous tissue and collagen fibers, and angiogenesis was observed in the first column cavity. At 4 weeks, new bone formation from the calvarial bone was showed on the first column cavity of the scaffold, and the lining osteocytes were observed along the new bone and the scaffold. In the 3 mm scaffold at 4 weeks, the angiogenesis and dense collagen bundle were observed on the second column cavity of the scaffold. The collagen bundle was showed higher density in 3 mm-scaffold compared with the 6 mm-scaffold (Figure 12).

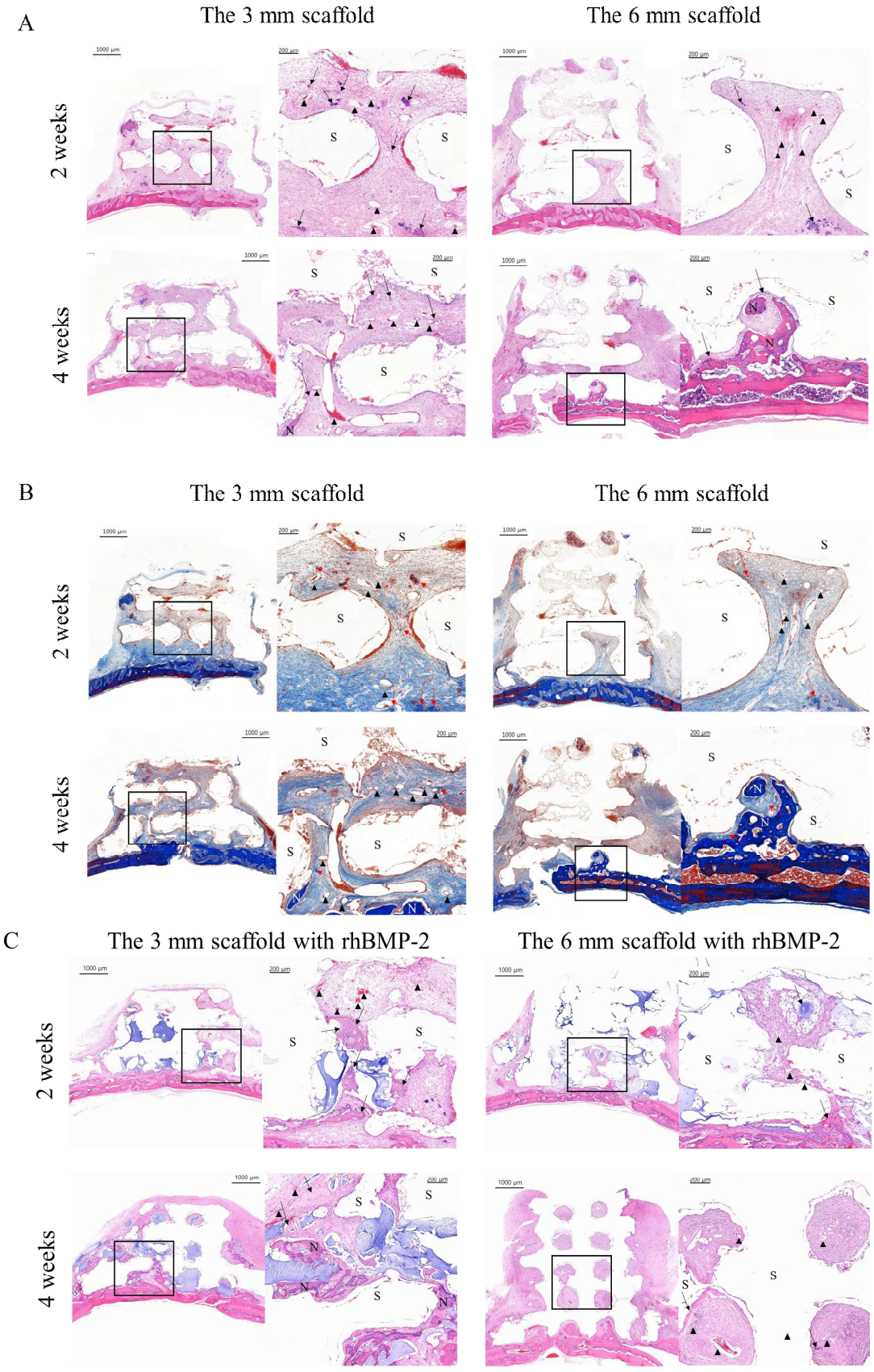
A
The 3 mm scaffold
The 6 mm scaffold
2 weeks
4 weeks
B
The 3 mm scaffold
The 6 mm scaffold
2 weeks
4 weeks
C
The 3 mm scaffold with rhBMP-2
The 6 mm scaffold with rhBMP-2
2 weeks
4 weeks

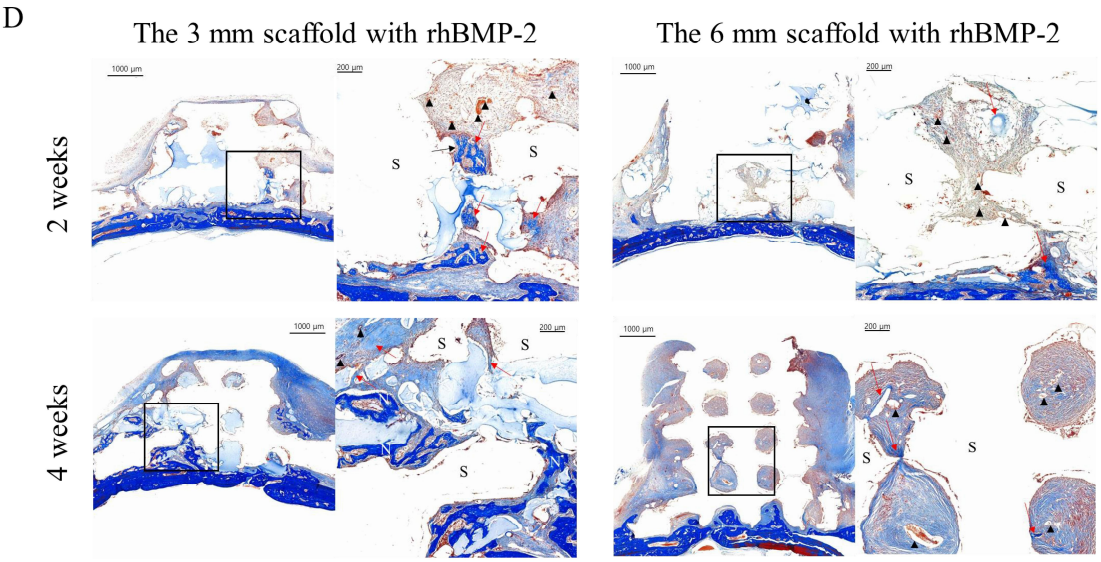


**Figure 12. Histological results of onlay graft with the 3D-printed customized kagome-structure PCL scaffold.** A. Hematoxylin and eosin staining of the scaffold. B. Masson's Goldner trichrome staining of the scaffold. The angiogenesis and dense collagen bundle were observed on the second column cavity of the scaffold. The collagen bundle was showed higher density in 3 mm-scaffold compared with the 6 mm-scaffold. New bone formation was observed at 4 weeks from the calvarial bone. C. Hematoxylin and eosin staining of the scaffold with rhBMP-2. D. Masson's Goldner trichrome staining of the scaffold with rhBMP-2. New bone formation was observed from 2 weeks from the calvarial bone with dominant angiogenesis and dense collagen bundle. The new bone, vessels and collagen bundles were showed higher density in 3 mm-scaffold compared with the 6 mm-scaffold.

S, Scaffold; N, New bone; Arrow showed New bone matrix, Arrow head showed new blood vessel.

**Discussion**

The surgical protocol of this study could successfully operate by covering non-damaged soft tissue over the 3 and 6 mm height of 3D printed kagome-structure PCL scaffold. One rat was showed wound dehiscence at postoperative 3 days, but there were no severe complications such as infection and graft failure of all rats. At 2 weeks, the 3 and 6 mm height of the scaffold was covered by fibrous tissue and successfully integrated with calvarial bone even after removal of fixation screws. New bone was grow up into the first column cavity of the scaffold as kagome-shape at 8 weeks after onlay graft, and the bone formation was similar aspect between the 3 and 6 mm height scaffold. With rhBMP-2 based on HA hydrogel, the new bone was formed at 2 weeks, and the height was comparable with the scaffold at 8 weeks. At 4 and 8 weeks, the 3 mm scaffold with rhBMP-2 was showed significant new bone formation in both of radiologically and histologically, but the 6 mm scaffold with rhBMP-2 was not showed superior results than the scaffold without rhBMP-2.

Onlay graft is difficult to successfully achieve due to the high risk of wound dehiscence and the nature of 1-wall defect. Autogenous bone has high potency of successful possibility for the onlay graft. [37-39] For successful outcome of bone graft, the graft should be well adapted to the native bone. Autograft often requires contouring the graft and native bone for intimate contact. Otherwise, any gaps between the native bone and the graft should be filled with other bone substitutes and covered with a resorbable membrane.[67] These process could be cause additional operation time and cost, and insufficient amount of bone by grinding the graft and bone. To overcome high rates of resorption in autograft bone and to avoid invasive surgery, many bone substitutes have been demonstrated. Alloplastic bone grafts, which are lack of osteoinduce and osteogenetic potential, usually showed slow and not sufficient bone formation in onlay graft [68, 69]. In clinically, general bone defects have complex curvatures and hardly achieve precise contact of the graft and the migration of osteoblasts and vascular cells for new bone formation.[70] In previous inlay graft in rabbit calvaria, the PCL-kagome scaffold showed excellent fitting ability and new bone formation capacity.[45] Unlike onlay graft, however, the inlay graft has optimal osteogenic conditions encircled by native bone and periosteum ensuring blood circulation to the enclosing tissue.[71]

Many researchers reported that the hexagonal kagome-structure were showed superior he mechanical properties and biological ability of cell proliferation compared with conventional grid structure.[45, 62, 72] Among several synthetic polymers fabrication of 3D printed scaffold such as poly(ε-caprolactone; PCL), poly(glycolic acid), poly(lactic acid)], and poly(lactic-coglycolic acid)[73-76]. PCL is a biodegradable polymer and widely used for its easy processability, excellent mechanical properties, and cell proliferation abilities.[43, 44] Kagome structure is one of the lightweight structures with high specific strength and stiffness [77], and has greater compressive and shear strength compared with tetrahedral and pyramidal structures.[78] The honeycomb structure has most stable mechanical properties among many lightweight structures, and the kagome structures are showed similar effective moduli and energy absorption properties with the honeycomb structures.[78] However, fabrication of 3D scaffold with kagome-structure was not widely conducted because it required complicated calculating process and mechanical engineering software. Since 2021, only three researches were conducted for bone graft scaffold with the kagome structure. One was published in 2019 that tricalcium phosphate scaffold with kagome structure used for bone regeneration possibility limited at cell culture level [72], and other two researches was our previous experiments with the PCL scaffold with kagome structure. [45, 62] In 2017, our first research was conducted for mechanical properties and cell-culture characteristics of kagome structure PCL scaffold.[62] A kagome-PCL scaffold was fabricated by additive manufacturing with a precision extruding deposition head (50 μm). The mechanical properties of kagome-structure scaffold were superior in compressive stiffness and mechanical bending properties to those of a grid-structure scaffold, and initial cell (Sarcoma osteogenic cells) attachment was enhanced due to the surface roughness of the kagome-structure scaffold. Further, the kagome-PCL scaffold was conducted in rabbit calvaria on the 8-shaped inlay defects in 2019.[45] The customized scaffold with complex morphology was successfully applied *in vivo* using 3D micro computed tomography. As a result, the 3D printed kagome-PCL scaffold showed excellent mechanical robustness and enhanced osteoconductivity than the grid-PCL scaffold. Therefore, the 3D printed kagome-structure scaffold can be tried for bone regeneration in unfavorable complex and large defects such as one-wall (onlay defect).

In our study, an intimate contact surface between the scaffold and calvarial bone was obtained by tightly fixing the wing of the scaffold, which had proper elasticity of the PCL. With regard our experimental result, a fibrous tissue did not intervene through the contact surface and it was indicated that the 3D-fabricated scaffold made closed contact with preventing fibrosis. On the other hand, new bone formation was not observed on micro-CT at 2 weeks. The drilling holes for decortification were small intra-osseous defects observed without regeneration. In histology results, connective tissues were filled into the cavity inside the scaffold, and new bone matrix and new blood vessel were observed in the first and second column cavity. At 4 weeks, the drilling holes were filled with new generated bone. New bone was observed inside the scaffold in the first column cavity, and new blood vessels were dominantly showed in the second column layer of the 3 mm scaffold compared with the 6 mm scaffold. At 8 weeks, we observed the kagome-shape new bone on first layer but there were no significantly difference between the 3 and 6 mm scaffold. Overall, total new bone formation height was about 1.0 mm with comparing the negative control. With considering the 0.5-1.0 mm thickness of rat calvarial bone subcutaneous tissue and skin, however, the new bone growth could be difficult to be naturally regenerated up to the top of both the 3 and 6 mm scaffolds. In addition, the mean new bone height with the 6 mm scaffold at 8 weeks (1.73 mm) was smaller than that of the 3 mm scaffold (2.13 mm) which was not observed aspect at 2 and 4 weeks. with regarding thin thickness of rat calvarial soft tissue, the scaffold of 6 mm in length could be excessive for maintain stable results for 8 weeks due to uncontrollable behavior of the rat.

The PCL—basis material for fabrication the scaffold in this study—has been widely used in field of tissue engineering and regenerative medicine.[79] Rui et al. reported the cartilage regeneration by using 3D scaffold of various gelatin/PCL ratio.[80] In 2017, Kim et al. presented a hybrid 3D cell-printing with PCL mesh to prevent contact of collagen during skin tissue maturation.[81] In 2019, Qian et al. reported the osteogenic and antimicrobial properties of PCL in oral tissue regeneration.[82] Thus, the PCL has been known to show excellent biocompatibility and regeneration capacity of soft tissues. With regard to our experimental results in term of soft tissue reaction, there were two important factors for onlay graft with the PCL scaffold. First, the optimal cell affinity of the PCL could allow to

preventing necrosis of overstretched skin without inflammatory reaction. Also, that was showed additional soft tissue augmentation effects regardless of the bone augmentation. Second, on the other hands, the fibrous tissue could be grow into the porous cavity of the kagome-PCL scaffold. This was showed positive effect for enhancing stability with fibrosis but was also negative effect, in terms of the onlay bone graft, to blockage the new bone growth. In conclusion, the kagome-PCL scaffold's combination structure of which was macroscopic kagome-structure and mesoscopic PCL porous structure was showed great possibility for optimal alloplastic bone substitutes. For successful clinical bone graft outcomes, the scaffold should be more increasing the regeneration capacity for rapid angiogenesis and osteogenic activity. Therefore, further study with growth factors such as rhBMP-2 should be conducted enhancing the osteogenic capacity. In addition, the Kagome PCL scaffold could be modified to maximizing the effect of the growth factors. The porosity, materials, and concentration of rhBMP-2 were necessary to optimize based on the ideal activity with considering the postulated kinetics of rhBMP-2.[83]

According to our surgical protocol, the scaffold could not be covered with periosteum which has osteogenic ability, and the new bone growth was showed from the calvarial bone. Therefore, for enhancing bone formation capacity in this one-wall defect reconstruction, it should be applied as osteoconductive carrier of bone growth factors (bone morphogenetic protein, fibroblast growth factor, insulin-like growth factor, vascular endothelial growth factor, etc). However, the hydrophobic characteristics of PCL scaffold could be disadvantaged for efficient incorporation of rhBMP-2. In 2007, the hydrogel was suggested for an effective carrier of rhBMP-2.[84] The cavity of 3D printed kagome-structure PCL scaffold could allow to stably contain the hydrogel incorporated rhBMP-2. In addition, 50% porosity and a sheet-like shape of the PCL-kagome scaffold could allow not only enhancing cell proliferation, but also slow releasing of the bone growth factors to promote regeneration capacity.[83] With regard bone formation on the scaffold with rhBMP-2, the new bone was significantly higher in the entire cavity of the scaffold compared with the scaffold without rhBMP-2, and the significance could be identified at postoperative 2 weeks with rhBMP-2 from at 8 weeks without rhBMP-2. However, quantitative measurement and comparison of new bone height could not be performed on CT images between the scaffold with and

without rhBMP-2 because the new bone was not only formed form the calvarial bone but also from the side of the scaffold with rhBMP-2.

Therefore, further onlay graft researches will be expected by this surgical protocol with 3D printed kagome-structure PCL scaffold with the hydrogel incorporated with rhBMP-2. The next step for clinical application of this scaffold with HA-based rhBMP-2 is to research releasing kinetics of rhBMP-2 with this scaffold, lowering the concentration of rhBMP-2, optimizing the porosity of the Kagome structure, 구조, 큰동물

**Conclusion**

For the onlay graft which is most difficult types of bone graft, our surgical protocol could avoid the scaffold exposure by covering non-damaged soft tissue over the scaffold and minimizing outside stitches and sufficient dissection without excessive tension of soft tissue. Also, careful drilling for decortification on thin calvarial bone could prevent excessive bleeding and hematoma. Therefore, this protocol could be expected to be able to apply onlay graft on rat calvarial bone.

Intimate contact surface could be obtained by fabricating the 3D scaffold with a PED head having a 50 μm nozzle. According to our experimental results, the 3D-kagome PCL scaffold was showed proper rigidity for enduring fixation and well integration with bone formation capacity. However, the new bone formation was limited on the first column layer of the kagome scaffold regardless of the scaffold's heights. Further studies should be conducted for application of growth factors on this scaffold to enhancing bone regeneration capacity.

**Reference**


1. Chiapasco M, C.P., Zaniboni M, *Bone augmentation procedures in implant dentistry.* Int J Oral Maxillofac Implants, 2009. **24 Suppl**: p. 237-259.
2. Aghaloo TL, M.P., *Which hard tissue augmentation techniques are the most successful in furnishing bony support for implant placement?* . Int J Oral Maxillofac Implants, 2007. **22(Suppl)**: p. 49-70.
3. Chiapasco M, T.G., Palombo D, et al. , *Dental implants placed in severely atrophic jaws reconstructed with autogenous calvarium, bovine bone mineral, and collagen membranes: A 3- to 19-year retrospective follow-up study.* Clin Oral Implants Res, 2018. **29**(7): p. 725-740.
4. Chiapasco M, Z.M., Rimondini L., *Autogenous only bone grafts vs. alveolar distraction osteogenesis for the correction of vertically deficient edentulous ridges: a 2-4-year prospective study on humans.* Clin Oral Implants Res, 2007. **18**: p. 432-440.
5. Park YJ, C.G., Jang JR, Jung SG, Han MS, Yu MG, Kook MS, Park HJ, Ryu SY, Oh HK, *The effect of new bone formation of onlay bone graft using various graft materials with a titanium cap on the rabbit calvarium.* J Korean Assoc Maxillofac Plast Reconstr Surg, 2009. **31**: p. 469-477.
6. Roccuzzo, M., et al., *Autogenous bone graft alone or associated with titanium mesh for vertical alveolar ridge augmentation: a controlled clinical trial.* Clin Oral Implants Res, 2007. **18**(3): p. 286-94.
7. Draenert FG, H.D., Neff A, Mueller WE, *Vertical Bone Augmentation Procedures: Basics and Techniques in Dental Implantology.* J Biomed Mater Res A, 2014. **102**: p. 1605-1613.
8. Schliephake, H., P. van den Berghe, and F.W. Neukam, *Osseointegration of titanium fixtures in onlay grafting procedures with autogenous bone and hydroxylapatite. An experimental histometric study.* Clin Oral Implants Res, 1991. **2**(2): p. 56-61.
9. Waasdorp, J. and M.A. Reynolds, *Allogeneic bone onlay grafts for alveolar ridge augmentation: a systematic review.* Int J Oral Maxillofac Implants, 2010. **25**(3): p. 525-31.
10. Draenert, F.G., et al., *Complications with allogeneic, cancellous bone blocks in*

*vertical alveolar ridge augmentation: prospective clinical case study and review of the literature.* Oral Surg Oral Med Oral Pathol Oral Radiol, 2016. **122**(2): p. e31-43.

11. BD, H., *Clinical and Histological Analysis of Different Types of Xenograft Bone Substitute for Alveolar Ridge Augmentation.* . Kim YK (Chairman), Bone Grafts for Implant Dentistry. The Korean Academy of Implant Dentistry, 2018. **37 (supple 2)**(14).
12. Keunyoung, J., et al., *Bone graft materials for current implant dentistry.* Journal of Dental Implant Research, 2020. **39**(1): p. 1-10.
13. SH, O., *Vertical alveolar bone augmentation using thin block and chip bone graft technique: Case report.* J Korean Assoc Maxillofac Plast Reconstr Surg, 2008. **30**: p. 108-113.
14. Merli, M., M. Migani, and M. Esposito, *Vertical ridge augmentation with autogenous bone grafts: resorbable barriers supported by ostheosynthesis plates versus titanium-reinforced barriers. A preliminary report of a blinded, randomized controlled clinical trial.* Int J Oral Maxillofac Implants, 2007. **22**(3): p. 373-82.
15. Proussaefs, P. and J. Lozada, *The use of intraorally harvested autogenous block grafts for vertical alveolar ridge augmentation: a human study.* Int J Periodontics Restorative Dent, 2005. **25**(4): p. 351-63.
16. Carini, F., et al., *Bone augmentation with TiMesh. autologous bone versus autologous bone and bone substitutes. A systematic review.* Annali di stomatologia, 2014. **5**(Suppl 2 to No 2): p. 27-36.
17. Figueiredo M, H.J., Martins G, Guerra F, Judas F, Figueiredo H, *Physicochemical characterization of biomaterials commonly used in dentistry as bone substitutes--comparison with human bone.* Journal of biomedical materials research. Part B, Applied biomaterials, 2010. **92**: p. 409-419.
18. Sakkas A, W.F., Heufelder M, Winter K, Schramm A, *Autogenous bone grafts in oral implantology-is it still a "gold standard"? A consecutive review of 279 patients with 456 clinical procedures.* Int J Implant Dent, 2017. **3**: p. 23.
19. Acocella A, B.R., Colafranceschi M, Sacco R. , *Clinical, histological and histomorphometric evaluation of the healing of mandibular ramus bone block grafts*

*for alveolar ridge augmentation before implant placement.* . J Craniomaxillofac Surg, 2010. **38**: p. 222-230.

20. Cordaro L, A.D., Cordaro M. , *Clinical results of alveolar ridge augmentation with mandibular block bone grafts in partially edentulous patients prior to implant placement.* Clinical oral implants research, 2002. **13**: p. 103-111.
21. Nyström E, A.J., Gunne J, Kahnberg KE, *10-year follow-up of onlay bone grafts and implants in severely resorbed maxillae.* International Journal of Oral and Maxillofacial Surgery, 2004. **33**: p. 258-262.
22. Misch CM, M.C., Resnik RR, Ismail YH. , *Reconstruction of maxillary alveolar defects with mandibular symphysis grafts for dental implants: a preliminary procedural report.* . The International journal of oral & maxillofacial implants, 1992. **7**: p. 360-366.
23. Galindo-Moreno P, L.-C.A., Ortega-Oller I, Monje A, O´ , Valle F, Catena A. , *Marginal bone loss as success criterion in implant dentistry: beyond 2 mm.* . Clinical oral implants research, 2015. **26**: p. e28-e34.
24. M., C., *How to reduce complications using autogenous bone blocks.* EAO 25th Annual Scientific Meeting. Congress Scientific Report, 2017: p. 10-11.
25. Kloss, F.R., V. Offermanns, and A. Kloss-Brandstätter, *CEComparison of allogeneic and autogenous bone grafts for augmentation of alveolar ridge defects-A 12-month retrospective radiographic evaluation.* Clinical oral implants research, 2018. **29**(11): p. 1163-1175.
26. Shet UK, C.M., Hur JW, Oh CJ, Chung K, Park HJ, Kook MS, Jung SG, Oh HK, *Evaluation of augmented alveolar bone and dental implant after autogenous onlay block bone graft.* J Korean Dent Assoc, 2012. **50**: p. 329-338.
27. Lee, H.J., et al., *Vertical alveolar ridge augmentation using autogenous bone grafts and platelet-enriched fibrin glue with simultaneous implant placement.* Oral Surg Oral Med Oral Pathol Oral Radiol Endod, 2008. **105**(1): p. 27-31.
28. Buser, D., et al., *Localized ridge augmentation using guided bone regeneration. II. Surgical procedure in the mandible.* Int J Periodontics Restorative Dent, 1995. **15**(1): p. 10-29.

29. Romanos, G.E., *Periosteal releasing incision for successful coverage of augmented sites. A technical note.* J Oral Implantol, 2010. **36**(1): p. 25-30.

30. Ogata, Y., et al., *Comparison of double-flap incision to periosteal releasing incision for flap advancement: a prospective clinical trial.* Int J Oral Maxillofac Implants, 2013. **28**(2): p. 597-604.

31. Greenstein, G., et al., *Flap advancement: practical techniques to attain tension-free primary closure.* J Periodontol, 2009. **80**(1): p. 4-15.

32. Hahn, J., *8-year onlay bone graft and ridge augmentation with PepGen P-15: a clinical and radiographic case study.* Implant Dent, 2004. **13**(3): p. 228-31.

33. Hartlev, J., et al., *Cone beam computed tomography evaluation of staged lateral ridge augmentation using platelet-rich fibrin or resorbable collagen membranes in a randomized controlled clinical trial.* Clin Oral Implants Res, 2019. **30**(3): p. 277-284.

34. Byun, H.Y. and H.L. Wang, *Sandwich bone augmentation using recombinant human platelet-derived growth factor and beta-tricalcium phosphate alloplast: case report.* Int J Periodontics Restorative Dent, 2008. **28**(1): p. 83-7.

35. Williams DF, B.J., Doherty PJ, *second consensus conference on defintions in biomaterials, in Dohery PJ et al. (Eds).* Biomaterial-Tissue interfaces. Advances in Biomaterials.

, 1992. **10, Elsevire, Amsterdam:525.**

36. Chung., S., *Hard tissue regeneration with synthetic scaffold - Synthetic(CaP) Bone.* Kim YK (Chairman) Bone Grafts for Implant Dentistry. The Korean Academy of Implant Dentistry. , 2018. **37 (supple 2)**(15).

37. Gomez-Barrena, E., et al., *A Multicentric, Open-Label, Randomized, Comparative Clinical Trial of Two Different Doses of Expanded hBM-MSCs Plus Biomaterial versus Iliac Crest Autograft, for Bone Healing in Nonunions after Long Bone Fractures: Study Protocol.* Stem Cells Int, 2018. **2018**: p. 6025918.

38. Gordh, M., et al., *Osteopromotive membranes enhance onlay integration and maintenance in the adult rat skull.* Int J Oral Maxillofac Surg, 1998. **27**(1): p. 67-73.

39. Mee-Rang, M., K. Myung-Rae, and K. Sun-Jong, *A RETROSPECTIVE STUDY OF THE SURGICAL SUCCESS AND VERTICAL BONE RESORPTION RATE AFTER*

*AUTOGENOUS BLOCK ONLAY GRAFT IN POSTERIOR MAXILLA.* Journal of the Korean Association of Oral and Maxillofacial Surgeons, 2009. **35**(5): p. 340-345.

40. Roseti, L., et al., *Scaffolds for Bone Tissue Engineering: State of the art and new perspectives.* Mater Sci Eng C Mater Biol Appl, 2017. **78**: p. 1246-1262.
41. Jammalamadaka, U. and K. Tappa, *Recent Advances in Biomaterials for 3D Printing and Tissue Engineering.* J Funct Biomater, 2018. **9**(1).
42. Thavornyutikarn, B., et al., *Bone tissue engineering scaffolding: computer-aided scaffolding techniques.* Prog Biomater, 2014. **3**: p. 61-102.
43. Kim, J.Y. and D.-W. Cho, *Blended PCL/PLGA scaffold fabrication using multi-head deposition system.* Microelectronic Engineering, 2009. **86**(4): p. 1447-1450.
44. Park, S.A., S.H. Lee, and W.D. Kim, *Fabrication of porous polycaprolactone/hydroxyapatite (PCL/HA) blend scaffolds using a 3D plotting system for bone tissue engineering.* Bioprocess Biosyst Eng, 2011. **34**(4): p. 505-13.
45. Lee, S.-H., et al., *Evaluation of mechanical strength and bone regeneration ability of 3D printed kagome-structure scaffold using rabbit calvarial defect model.* Materials Science and Engineering: C, 2019. **98**: p. 949-959.
46. Lang, N.P., *Focus on intrabony defects--conservative therapy.* Periodontol 2000, 2000. **22**: p. 51-8.
47. Kim, Y., T.K. Kim, and D.H. Leem, *Clinical Study of a Flap Advancement Technique Without Vertical Incision for Guided Bone Regeneration.* Int J Oral Maxillofac Implants, 2015. **30**(5): p. 1113-8.
48. Murata M, A.T., Mitsugi M, Kabir MA, Minamida Y, Um IW, Minamida Y, Kim KW, Kim YK, Sun Y, Qin C, *Autograft of dentin materials for bone regeneration.* In: Pignatello R, editor. Advances in Biomaterials Science and Biomedical Applications. Croatia: InTech Publisher, 2013. pp. 391-403.: p. 391-403.
49. Burkus, J.K., H.S. Sandhu, and M.F. Gornet, *Influence of rhBMP-2 on the healing patterns associated with allograft interbody constructs in comparison with autograft.* Spine (Phila Pa 1976), 2006. **31**(7): p. 775-81.
50. Lee, S.H. and H. Shin, *Matrices and scaffolds for delivery of bioactive molecules in bone and cartilage tissue engineering.* Adv Drug Deliv Rev, 2007. **59**(4-5): p. 339-

59.

51. Haidar, Z.S., R.C. Hamdy, and M. Tabrizian, *Delivery of recombinant bone morphogenetic proteins for bone regeneration and repair. Part B: Delivery systems for BMPs in orthopaedic and craniofacial tissue engineering.* Biotechnol Lett, 2009. **31**(12): p. 1825-35.

52. Welch, R.D., et al., *Effect of recombinant human bone morphogenetic protein-2 on fracture healing in a goat tibial fracture model.* J Bone Miner Res, 1998. **13**(9): p. 1483-90.

53. Magin, M.N. and G. Delling, *Improved lumbar vertebral interbody fusion using rhOP-1: a comparison of autogenous bone graft, bovine hydroxylapatite (Bio-Oss), and BMP-7 (rhOP-1) in sheep.* Spine (Phila Pa 1976), 2001. **26**(5): p. 469-78.

54. Cook, S.D., et al., *Effect of recombinant human osteogenic protein-1 on healing of segmental defects in non-human primates.* J Bone Joint Surg Am, 1995. **77**(5): p. 734-50.

55. Boyne, P.J., *Animal studies of application of rhBMP-2 in maxillofacial reconstruction.* Bone, 1996. **19**(1 Suppl): p. 83s-92s.

56. Bouxsein, M.L., et al., *Recombinant human bone morphogenetic protein-2 accelerates healing in a rabbit ulnar osteotomy model.* J Bone Joint Surg Am, 2001. **83-a**(8): p. 1219-30.

57. Wozney, J.M., *Overview of bone morphogenetic proteins.* Spine (Phila Pa 1976), 2002. **27**(16 Suppl 1): p. S2-8.

58. Seeherman, H., J. Wozney, and R. Li, *Bone morphogenetic protein delivery systems.* Spine (Phila Pa 1976), 2002. **27**(16 Suppl 1): p. S16-23.

59. Kempen, D.H.R., et al., *Retention of in vitro and in vivo BMP-2 bioactivities in sustained delivery vehicles for bone tissue engineering.* Biomaterials, 2008. **29**(22): p. 3245-3252.

60. Um, I.-W., et al., *Postulated release profile of recombinant human bone morphogenetic protein-2 (rhBMP-2) from demineralized dentin matrix.* J Korean Assoc Oral Maxillofac Surg, 2019. **45**(3): p. 123-128.

61. Kim, J., et al., *Bone regeneration using hyaluronic acid-based hydrogel with bone*

*morphogenic protein-2 and human mesenchymal stem cells.* Biomaterials, 2007. **28**(10): p. 1830-1837.

62. Lee, S.H., et al., *Mechanical properties and cell-culture characteristics of a polycaprolactone kagome-structure scaffold fabricated by a precision extruding deposition system.* Biomed Mater, 2017. **12**(5): p. 055003.
63. Greenstein, G., et al., *The role of bone decortication in enhancing the results of guided bone regeneration: a literature review.* J Periodontol, 2009. **80**(2): p. 175-89.
64. Kim, J., et al., *Bone regeneration using hyaluronic acid-based hydrogel with bone morphogenic protein −2 and human mesenchymal stem cell.* Biomaterials, 2007. **28**: p. 1830-7.
65. Jin, I.G., et al., *Effect of bone marrow-derived stem cells and bone morphogenetic protein-2 on treatment of osteoradionecrosis in a rat model.* J Craniomaxillofac Surg, 2015. **43**(8): p. 1478-86.
66. Hong, S.R., et al., *Biocompatibility and biodegradation of cross-linked gelatin/hyaluronic acid sponge in rat subcutaneous tissue.* J Biomater Sci Polym Ed, 2004. **15**(2): p. 201-14.
67. Louis, P.J. and S. Sittitavornwong, *Managing Bone Grafts for the Mandible.* Oral Maxillofac Surg Clin North Am, 2019. **31**(2): p. 317-330.
68. el Deeb, M. and R.E. Holmes, *Zygomatic and mandibular augmentation with proplast and porous hydroxyapatite in rhesus monkeys.* J Oral Maxillofac Surg, 1989. **47**(5): p. 480-8.
69. Salyer, K.E. and C.D. Hall, *Porous hydroxyapatite as an onlay bone-graft substitute for maxillofacial surgery.* Plast Reconstr Surg, 1989. **84**(2): p. 236-44.
70. Temple, J.P., et al., *Engineering anatomically shaped vascularized bone grafts with hASCs and 3D-printed PCL scaffolds.* Journal of Biomedical Materials Research Part A, 2014. **102**(12): p. 4317-4325.
71. Felice, P., et al., *Inlay versus onlay iliac bone grafting in atrophic posterior mandible: a prospective controlled clinical trial for the comparison of two techniques.* Clin Implant Dent Relat Res, 2009. **11 Suppl 1**: p. e69-82.
72. Schmidleithner, C., et al., *Application of high resolution DLP stereolithography for*

*fabrication of tricalcium phosphate scaffolds for bone regeneration.* Biomed Mater, 2019. **14**(4): p. 045018.

73. Boland, E.D., et al., *Utilizing acid pretreatment and electrospinning to improve biocompatibility of poly(glycolic acid) for tissue engineering.* Journal of Biomedical Materials Research Part B: Applied Biomaterials, 2004. **71B**(1): p. 144-152.
74. Serra, T., J.A. Planell, and M. Navarro, *High-resolution PLA-based composite scaffolds via 3-D printing technology.* Acta Biomaterialia, 2013. **9**(3): p. 5521-5530.
75. Bose, S., S. Vahabzadeh, and A. Bandyopadhyay, *Bone tissue engineering using 3D printing.* Materials Today, 2013. **16**(12): p. 496-504.
76. Chia, H.N. and B.M. Wu, *High-resolution direct 3D printed PLGA scaffolds: print and shrink.* Biofabrication, 2014. **7**(1): p. 015002.
77. Gautam, R. and S. Idapalapati, *Performance of strut-reinforced Kagome truss core structure under compression fabricated by selective laser melting.* Materials & Design, 2019. **164**: p. 107541.
78. Hyun, S., et al., *Simulated properties of Kagomé and tetragonal truss core panels.* International Journal of Solids and Structures, 2003. **40**(25): p. 6989-6998.
79. Han, F., et al., *Tissue Engineering and Regenerative Medicine: Achievements, Future, and Sustainability in Asia.* Frontiers in bioengineering and biotechnology, 2020. **8**: p. 83-83.
80. Zheng, R., et al., *The influence of Gelatin/PCL ratio and 3-D construct shape of electrospun membranes on cartilage regeneration.* Biomaterials, 2014. **35**(1): p. 152-64.
81. Kim, B.S., et al., *Direct 3D cell-printing of human skin with functional transwell system.* Biofabrication, 2017. **9**(2): p. 025034.
82. Qian, Y., et al., *Triple PLGA/PCL Scaffold Modification Including Silver Impregnation, Collagen Coating, and Electrospinning Significantly Improve Biocompatibility, Antimicrobial, and Osteogenic Properties for Orofacial Tissue Regeneration.* ACS Appl Mater Interfaces, 2019. **11**(41): p. 37381-37396.
83. Um, I.W., et al., *Postulated release profile of recombinant human bone morphogenetic protein-2 (rhBMP-2) from demineralized dentin matrix.* J Korean

Assoc Oral Maxillofac Surg, 2019. **45**(3): p. 123-128.

84. Kim, J., et al., *Bone regeneration using hyaluronic acid-based hydrogel with bone morphogenic protein-2 and human mesenchymal stem cells.* Biomaterials, 2007. **28**(10): p. 1830-7.

국문요약

악골의 결손부나 미용 등의 목적으로 악골의 골이식이 필요한 경우가 많다. 그러나 onlay 형태의 one-wall 결손부 재건은 부적합한 혈행공급과 이식재의 불안정으로 인해 좋은 결과를 얻는 것이 매우 어렵다. Onlay 형태의 골이식이 성공하기 위해서는 골재생능력이 좋은 골이식재의 선택과 창상열개와 같은 합병증을 최소화 할 수 있는 수술법이 모두 중요하다. 최근에 주목받고 있는 3 차원적으로 디자인된 Kagome 구조의 PCL 담체는 골내 결손부에서 성공적인 골전도 능력이 보고되었다. 또한 이 담체는 엄격한 고정이 될 수 있을 정도의 적절한 견고성, 수여부와 긴밀한 접촉면을 만들 수 있는 3 차원적 디자인, 그리고 생체적합성을 가진다. 따라서 이 담체는 가장 성공하기 어려운 onlay 형태의 골이식을 시도할 수 있는 적절한 조건을 갖췄다. 한편, Onlay 형태의 graft 의 가장 호발하는 합병증은 연조직 양의 부족으로 인한 창상열개, 절개선 상에 포함된 상부 연조직으로부터의 부족한 혈행공급 등이 있다. 본 연구에서는 쥐 두개골의 CT 데이터의 두개골의 곡면을 따라서 만든 높이 3, 6 mm, 직경 5mm 의 원통형 Kagome 구조의 PCL 담체를 이용하여 합병증을 최소화한 onlay 형태의 골이식 수술 방법을 소개하고, 하이루론산 (HA) 기반의 사람재조합골형성단백질 (rhBMP-2)를 적용한 골이식의 결과를 보고하고자 한다.

수술기법으로 절개선은 이식편 위에 오지 않도록 담체의 후방에 가해지고, 전방으로 충분히 박리한 후 Bregma 에 피질골제거를 위한 구멍을 만들고, 4 개의 미니스크류를 이용하여 단단히 고정한다. 3, 6 mm 의 담체를 이식한 쥐는 2 주, 4 주 8 주에 희생한다. 각 군당 4 마리씩, 총 24 마리의 쥐의 모든 수술부위는 담체의 노출 없이 치유되었다. 각 주차 별 희생 후, 모든 담체는 고정 스크류 제거 후에도 잘 생착되었다. Micro-CT 에서 2 주차에는 신생골 형성이 관찰되지 않았지만, 8 주차에 담체 첫번째 층 공간에 kagome 형태의 신생골이 형성되었고, 대조군과 비교했을 때 이식한 담체 내부의 평균 골형성 높이는 약 1.0 mm 였다. 조직학적으로 담체의 빈 공극에 신생혈관과 콜라겐이 2 주차에 자라들어온 것이 확인되었다. 4 주차에 두개골에서부터 골형성이 시작되었고 명확한 신생골이 관찰되었다. HA 기반의 rhBMP-2 (1.0 mg/mL)을 적용할 때, 2 주차의 신생골형성과 신생혈관형성, 콜라겐의 농도는 rhBMP-2 를 적용하지 않은 8 주차의 결과와 비견할 만큼의 결과를 보였다. 특히, 4 주와 8 주차에 rhBMP-2 를 적용한 3 mm 의 담체는 6 mm 의 담체에 비해 우월한 골형성 결과를 보였다.

우리 연구 결과에 따르면, 이 3 차원 Kagoma 구조의 PCL 담체는 onlay graft 에서 고정을 얻기 충분한 물리적 특징과 골전도능을 보였고, 특히 Kagome 의 macrostructure 와 PCL 의 mesostructure 가 효과적인 세포 반응을 이끌어 낸 것로 보인다. 이 담체에 HA hydrogel 과 rhBMP-2 를 적용하면 2 주차에 조기 골형성을 보였고, 그 형성량은 rhBMP-2 를 적용하지 않은 8 주차의 결과와 비견할 했다. 따라서 이 담체와 여기에 적용된 HA hydrogel 은 rhBMP-2 의 적합한 운반체임을 나타낸다. 골 형성능력을 증진시키 위해서, 이 담체에 rhBMP-2 의 가장 이상적인 적용에 대한 추가적인 연구가 큰 동물을 대상으로 필요할 것으로 보인다.

중심단어: 골이식, 온레이 골이식, PCL, 재조합 인간 골 형성 단백질-2, 담체, 조직공학